



Geospatial input data for the PALM model system 6.0: model requirements, data sources, and processing

Wieke Heldens¹, Cornelia Burmeister³, Farah Kanani-Sühring^{2,4}, Björn Maronga^{2,5}, Dirk Pavlik³, Matthias Sühring², Julian Zeidler¹, and Thomas Esch¹

¹Deutsches Zentrum für Luft- und Raumfahrt, Earth Observation Center, Land Surface Dynamics, Oberpfaffenhofen, Germany

²Institute of Meteorology and Climatology, Leibniz University Hannover, Hannover, Germany

³GEO-NET Environmental Services GmbH, Hannover, Dresden, Germany

⁴Harz Energie GmbH & Co. KG, Goslar, Germany

⁵Geophysical Institute, University of Bergen, Bergen, Norway

Correspondence: Wieke Heldens (wieke.heldens@dlr.de)

Abstract. The PALM model system 6.0 is designed to simulate micro- and mesoscale flow dynamics in realistic urban environments. The simulation results can be very valuable for various urban applications, for example to develop and improve mitigation strategies related to heat stress or air pollution. For the accurate modelling of urban environments, realistic boundary conditions need to be considered for the atmosphere, the local environment, and the soil. The local environment with its geospatial components is described in the static driver of the model and follows a standardized, hereafter called PALM input data standard. The main input parameters describe surface type, buildings and vegetation. Depending on the desired simulation scenario and the available data, the local environment can be described at different levels of detail. To compile a complete static driver describing a whole city, various data sources are used, including remote sensing, municipal data collections and open data such as OpenStreetMap. This manuscript shows how input data sets for three German cities can be derived. Based on these data sets, the static driver for PALM can be generated. As the collection and preparation of input data sets is tedious, prospective research aims at the development of a semi-automated processing chain to support users in formatting their geospatial data.

1 Introduction

Nowadays, computational fluid dynamic models are increasingly used to simulate the atmospheric flow within urban environments, e.g., to develop and improve mitigation strategies for heat stress (e.g. Sharma et al., 2018) or air pollution scenarios (e.g. Kurppa et al., 2018). In order to draw a realistic picture of the thermodynamic and dynamic conditions within urban environments, it is required to consider and sufficiently represent all the relevant physics on the micro- and meso-scale, as well as realistic boundary conditions to reflect the real-world conditions. Besides realistic initial and boundary conditions for



the atmosphere and the soil, it is crucial to have detailed information on the local environment as well, i.e., terrain height, building and street canyon geometries and surface properties, as well as the type and the current state of the plant canopy, in order to accurately represent the real-world conditions within the urban canopy layer. For instance, detailed information on the geometry of the surrounding buildings and the nearby street canyons is inevitable to study ventilation and air pollution in street
5 canyons (Lo and Ngan, 2017) or within courtyard cavities (Gronemeier and Sühling, 2019), or to assess the nighttime fresh-air supply by cold-air drainage flows within residential areas.

The PALM model system 6.0, a large-eddy simulation-based code including several components for urban micro-scale simulation, allows the simulation of urban micro climate of realistic urban environments, as it is capable of handling detailed information on the real-world environment (Maronga et al., 2019). Using such a model, however, implies that the amount and
10 requirements of input data drastically increases compared to simplified scenario studies. The main objective of this paper is therefore to describe the extensive model requirements, data sources and processing of the geospatial input data for PALM 6.0. This paper focuses on the geospatial input data only, which is required to create suitable input files for PALM and that describe the (static) information, representing the local environment and surface boundary conditions for the model. This is a key aspect in the numerical simulation of urban flows since they determine the atmosphere-surface exchange of momentum,
15 heat and moisture.

The paper starts with a description of the input data requirements of PALM (Sect. 2). Data availability, including possibilities and limitations of a wide range of suitable data sources to satisfy these needs are described in Sect. 3. Each of these data sources require its individual pre-processing to make the data fitting to the model input requirements. In Sect. 4 it is demonstrated exemplary how this pre-processing can be realized for three German cities. In Sect. 5 it is described how the input data
20 is prepared for PALM. The paper concludes with a discussion of the input data and existing challenges that are related to collecting and preparing the input data according to the PALM input data standard.

2 Input data requirements by PALM

The geospatial input data for PALM is organised hierarchically, with a set of minimum requirements and further optional input data, depending on the objective of the simulation and available input data. This section gives a description of the input data
25 requirements of PALM in the different situations as well as a short description of the required parameters.

2.1 Requirements and hierarchy

All geospatial input data is provided by the user in a netCDF driver file (hereafter referred to as static driver) that comprises all static (i.e., time-invariant) spatial information as well as metadata according to the so-called PALM input data standard (PIDS, see Appendix A). The PIDS inherits most of the netCDF Climate and Forecast Metadata Conventions Version 1.7
30 (CF-1.7)¹ and is therefore also conform with the conventions of the Cooperative Ocean/Atmosphere Research Data Service

¹cfconventions.org/Data/cf-conventions/cf-conventions-1.7/cf-conventions.html



(COORDS)². Depending on the setup (e.g., only dynamic flow or fully thermodynamic simulation with interactive surfaces) there is a minimum set of mandatory variables and several optional ones that need to be included in the static driver.

The initialization in PALM follows a multi-step approach, depending on the given level of detail (LOD) of each variable as provided in the static input file. In absence of a static driver, i.e., the lowest level of detail, LOD 0, a horizontally homogeneous surface is initialized based on settings using Fortran NAMELIST parameters, e.g., homogeneously vegetated surfaces and surface properties in the land-surface model (see Maronga et al., 2019). In LOD 1, surface information is passed to PALM via two-dimensional fields in the static driver. Table 12 gives an overview of all LOD1 fields that can be read by PALM. For simulations without thermodynamics, i.e., when no interactive surface schemes are used, only the fields `zt` (terrain height) and `buildings_2d` (building height) are used for initialization and at least one of these fields must be provided. Additionally, the field for the building identifier (ID) `building_id` must be set when `zt` is used in order to guarantee a correct mapping of buildings on the terrain (see Sect. 5.2 for details). As the static driver contains rastered data, information about objects that extent over several grid volumes is lost. By using an ID field this information can be retained. Note that `building_id` is thus also needed when the building-based indoor model of PALM is switched on (see Maronga et al., 2019). For cases with interactive surfaces, each surface element is classified according to its treatment, i.e., default- (i.e., non-interactive), land surface- or urban-type (i.e., building). In setups without interactive surfaces, all surface elements are classified as default-type. In setups with interactive surfaces, a surface classification using the fields `vegetation_type`, `water_type`, `pavement_type`, and `building_type` is utilised (see Sect. 2.6). Currently, each surface pixel (y, x) must be assigned to one of the aforementioned types. In the future, PALM will also allow a tile approach so that multiple types can be present in one grid box, which will be particularly useful when using coarser grid spacings (> 10 m), where neglecting sub-pixel heterogeneity is no longer adequate. The tile approach will be realized by specifying the individual portions via the field `surface_fraction`, which is already recognized by PALM.

By setting the surface types, all required parameters for the surface treatment are automatically set to default values. Note that pavement- and land vegetation-type surface require the setting of `soil_type` at the respective pixels. When using the surface classification, a default albedo type is automatically set for each pixel depending on the chosen surface classification. This can, however, be overwritten using the optional field `albedo_type`. Tables A1-A7 in the Appendix give an overview of the classifications used and the parameters automatically set when using LOD1.

Based on the LOD1 classification of each surface pixel, the static driver allows to overwrite all or selected parameters that were automatically set by the LOD1 input data (for example roughness lengths, surface emissivity, etc., see Tables A1-A7 in the Appendix). For each `*_type` field in LOD1 there is thus a respective `*_pars` field, representing LOD2 data (see Table 13). Note that LOD2 can only be used when simultaneously having specified LOD1 data. The `*_pars` fields then can contain fill values except for those locations where the data should be overwritten by LOD2 input data. Additionally, LOD2 offers the `NC_BYTE` field `buildings_3d`, which can be used to specify three-dimensional building structures including overhanging structures, thoroughfares, and bridges (see Sect. 2.5). Unlike for the other `*_pars` fields, the LOD1

²see ferret.pmml.noaa.gov/Ferret/documentation/coards-netcdf-conventions



data (i.e., `buildings_2d`) is not used if LOD2 data (i.e., `buildings_3d`) is present in the data. Furthermore, the field `root_fraction` can be set in order to specify a different vertical root distribution in the soil model of the parameterized vegetation in the land surface model.

While LOD2 is limited to a localized setting of individual surface or material properties based on location (y, x) only, LOD3 and LOD4 settings (see Tables. 14 and 15) allow an even more detailed specification of building parameters. Note that in LOD4, the input data no longer depends on the rastered PALM grid, but is arranged in a one-dimensional array of size ns , where ns is the number of surface elements on the model domain. For each surface element, the user then has to specify the position of the surface element in the PALM domain space, i.e., $(z(1:ns), y(1:ns), x(1:ns))$ as well as the orientation of surface elements in terms of azimuth and zenith angles ($azimuth(1:ns)$ and $zenith(1:ns)$, respectively) in one-dimensional fields.

Additionally, three-dimensional fields of leaf-area density, LAD (`lad`), and basal-area density, BAD (`bad`), as well root fractions (`root_fraction_resolved`) and a tree ID (`tree_id`) can be used to set-up resolved-scale plant canopies (see Sect. 5.3).

2.2 Geo-referencing

Various model components such as the radiation parametrization, the representation of the Coriolis force or geo-referencing of model output require information about the geo-location of the grid cells of PALM. Therefore, the static input file must contain information about the longitude and latitude, as well as the Easting and Northing UTM coordinates of the lower-left corner of the model domain. Furthermore, reference height of the lowest model grid point as well as the rotation angle of the model domain must be provided, which is especially important to setup virtual measurement positions and trajectories within the model according to 'real-world' measurements (Maronga et al., 2019). The required coordinate information must be given as global attributes in the NetCDF file.

2.3 Terrain height

To consider effects of elevation changes on the flow, the terrain height z_t can be provided for each discrete (y, x) -location in the model. Data gaps leading to fill values are forbidden. In case z_t is not provided, the land surface is set-up at $z = 0$ m.

The z_t can be provided in absolute values, i.e., in meters above sea level, or in relative heights where, e.g., its minimum value is already subtracted. If absolute values are used, PALM will subtract the minimum value within the domain itself to save computational grid points (no computations are needed within the soil). At this point we note that the original terrain height might be further processed and slightly modified by PALM to fulfill certain requirements, which is described in detail in Sect. 5.2.



2.4 Surface classification

In order to parameterize atmosphere-surface-interactions, PALM needs to solve the energy balance at physical surfaces. For doing this, several physical surface parameters such as the heat capacity, roughness, albedo, emissivity, information about vegetation, etc., must be known. To allow for proper LOD1 initialization of material parameters and surface properties via pre-defined lists, PALM classifies all horizontal and vertical surfaces in the model according to their general type, e.g., whether it is a building or a vegetation surface. PALM considers four different types of surfaces: building, vegetation, pavement and water surfaces, while the surfaces are classified in a two-step approach. In a first step, grid points are flagged as atmosphere, building or terrain grid point. Surfaces which belong to a building grid point are automatically flagged as building surfaces, while surfaces which belong to a terrain grid point are flagged as land surfaces. In a second step, surfaces are further specified according to their respective type, which enables proper LOD 1 initialization with pre-defined lists for material and surface properties. For this reason, input of `building_type`, `vegetation_type`, `pavement_type` and `water_type` is required. At each (y, x) -location at least one of these types must have a non-missing value, so that each surface element can be classified appropriately, either as a pavement, vegetation, or water. It is also required that the given `*_type` matches with the general classification into building- and land-surface, i.e., at locations where buildings (see Sect. 2.5) are defined also `building_type` must be defined, while at land-surfaces at least one one of `vegetation_type`, `pavement_type` or `water_type` must be defined.

2.5 Buildings

Information on the location and height of buildings can be provided as two-dimensional buildings heights (`buildings_2d`, LOD 1) or as a three-dimensional integer array (`buildings_3d`, LOD 2), where each building (non-building) grid point is masked by 1 (0). At locations where no buildings are located, `buildings_2d` may contain fill values, while `buildings_3d` must not contain any fill values. In the LOD 1 case, buildings are always mounted on the Earth's surface and overhanging structures such as tunnels or bridges are not allowed, while in the LOD 2 case also overhanging obstacles are allowed. In both cases, building information is given relative to the terrain height and buildings are mapped onto the top of the terrain during model initialization, which is described in detail in Sect. 5.2. At this point we note that PALM can also consider bridges, which can be input as three-dimensional building structures but require a special treatment as further discussed in Sect. 5.2.

To distinguish between single buildings, e.g., in order to map them accordingly onto the underlying terrain (please see Sect. 5.2), or to compute the energy demand of single buildings (Maronga et al., 2019), each building has an unique identification number (`building_id`) that must be given in the static input file at each (y, x) -location where `buildings_2d` or `buildings_3d` is defined.

Further, in case the energy balance for building surfaces should be solved (Resler et al., 2017; Maronga et al., 2019), information on the type of the buildings must be provided. To solve the energy balance at building surfaces appropriately, various wall material and surface properties must be known, e.g., wall thicknesses, heat capacities and conductivities, window and wall fractions, albedo, etc. which depend on the individual construction parameters and the current state of building restora-



tion. As many of these information are quite often unknown, buildings are classified into characteristic types in order to use default parameters. For this, buildings are classified according to their year of construction and its general usage (residential or office building). PALM provides lists of wall material and surface parameters for six building types: 1 - residential buildings build before 1950, 2 - residential buildings build between 1951 and 2000, 3 - residential buildings build after 2001, 4 - office buildings build before 1950, 5 - office buildings build between 1951 and 2000, and 6 - office buildings build after 2001, and 7 - bridges. At this point we note that `building_type = 7` is exclusively used to identify bridges and to distinguish them from other three-dimension building structures. The respective `building_type` must be provided for each discrete (y, x) -location where `building_2d` or `building_3d` is defined. Even though building parameters are difficult to aggregate in practice, PALM nevertheless allows to prescribe different types defined among a single building, e.g., to consider building extensions with different physical properties or different usage in case such information is available. In addition, to modify wall material and surface parameters at different (y, x) -location or even at single surface elements, `building_pars` or `building_surface_pars`, respectively, can be optionally provided.

2.6 Land surfaces

Beside the general classification via pre-defined parameter lists for each land-surface type, physical surface parameters can be further specified with `vegetation_pars`, `water_pars` or `pavement_pars`, which can be optionally provided, as explained in Sect. 2.1.

2.6.1 Vegetation

PALM distinguishes between parameterized vegetation that is not resolved by the numerical grid and thus considered flat (e.g., short grass), and tall vegetation that can be partially resolved by the numerical grid, depending on the grid spacing used (e.g., shrubs or trees). Parameterized vegetation is considered within the energy balance solver for land surfaces, where the given `vegetation_type` defines the physical properties at the respective surface element. These can optionally be specified in more detail by `vegetation_pars`, which may contain missing values for single parameters and locations, and the respective properties are only updated and customized where they contain non-missing values, i.e., it is allowed to provide parameters only at locations where these are available. At parameterized vegetation surfaces, additional information concerning the root-area-density distribution (`root_area_dens_s`) within the soil can be optionally provided. If it is not provided it is taken from bulk parameter lists defined by the given `vegetation_type`.

In contrast to parameterized vegetation, resolved vegetation directly accounts for a sink term in the momentum equations (e.g. Kanani-Sühring and Raasch, 2015) and directly affects its surroundings via shading and three-dimensional reflections (Resler et al., 2017). To consider these effects in the model, information about the leaf-area density (LAD) within the respective grid volumes is required and can be input via `LAD`, which is mapped on top of the underlying terrain. The leaf-area density in the model is initialized at every location where `LAD` has non-missing and positive values, elsewhere it is set to zero.



2.6.2 Pavements

Pavement surfaces can be specified via `pavement_type` which defines the surface and subsurface material properties via pre-defined parameter lists. To further specify pavement parameters, `pavement_pars` and `pavement_subsurface_pars` can be optionally provided for defining surface and sub-surface parameters, respectively.

- 5 Also, it is possible to provide additional input for street types and street crossings with `street_type` and `street_crossing`, respectively. The street-type classification can be used by PALM to parameterize traffic emissions within the embedded chemistry model, while both the street network and crossings may in the future be employed by the embedded multi-agent system for urban residents (Maronga et al., 2019).

2.6.3 Water bodies

- 10 Water surfaces can be specified via `water_type` which defines the surface properties via pre-defined parameter lists. To further specify water surface parameters, `water_pars` can be optionally provided.

2.7 Soil classification

- To consider the interaction of the land surface with the underlying soil at vegetation- and pavement surfaces, a `soil_type` must be given at grid cells that are classified as vegetation or pavement surfaces, defining a list of default physical parameters for pre-defined soil types. `soil_type` can be given for different level of detail. For LOD1, `soil_type` must be provided for each (y, x) -location where vegetation or pavement is defined, assuming that soil properties are vertically homogeneous, while for LOD2 `soil_type` is given for each (z_{soil}, y, x) -location, with z_{soil} being the depths of the soil layers, in order to consider variations of soil properties also in the vertical direction. To further customize physical soil parameters, `soil_pars` can be optionally provided either as LOD 3 to provide vertically homogeneous parameters, or as LOD 4 to provide vertically heterogeneous parameters, i.e., each soil layer at each relevant surface element can be given individual physical properties. `soil_pars` may contain missing values and is only used to update the physical soil parameters at locations and for parameters that are non-missing, i.e., it is allowed to provide only single parameters at locations where this information is available.

2.8 Surface albedo

- Information concerning the albedo for the different surfaces is already given within the pre-defined parameter lists for building and land-surfaces. However, more detailed information concerning the `albedo_type` (predefined list of broadband and spectral albedos for direct and diffuse radiation) or broadband / spectral surface albedos at each (y, x) -location (`albedo_pars`) can be provided optionally.



3 Data sources

Masson et al. (2020) review various data sources for urban climate models at meso- and micro-scale. The requirement of a spatial resolution of 1 - 10 m for building-resolving simulations, being a key focus of PALM, reduces the available sources of data significantly. The most important sources are remote sensing, governmental/municipal data and open data, as they allow
5 area-wide and automated pre-processing, while field surveys and manual mapping are only a practicable option for small areas of interest, e.g. of one building block in a city. Often, a combination of different sources is required to achieve a consistent coverage with detailed information for the entire area of interest.

The observation of the characteristics and dynamics of the Earth's surface by means of remote sensing has become increasingly important in recent years. In general, remote sensing approaches take advantage of the fact that material- or object-specific
10 interactions occur between the surface and land cover type on the one hand, and the electromagnetic radiation interacting with them on the other hand. This specific spectral signature or back-scattering pattern can then effectively be used to identify and discriminate different surface and material types. Active imaging systems such as radar or laser scanners carry their individual radiation sources (Baghdadi and Zribi, 2016). The intensity and pattern of the backscattering then allows mapping the position, type and, in case of laser scanners, height of surfaces and objects. This can be used to create digital surface models, e.g., based
15 on the radar satellite TerraSAR-X at a global scale (Rizzoli et al., 2017) or at local scale using airborne LiDAR systems (Yan et al., 2015). Optical remote sensing makes use of the reflected radiation of the sun. There is a broad range of systems available, mounted on satellite platforms as well as airborne and UAV-mounted sensors. The selection of the sensor used depends on spectral characteristics, spatial resolution, availability for the area of interest and costs. Typical mapping tasks carried out with optical remote sensing are land cover mapping (e.g. Khatami et al., 2016; Wulder et al., 2018) and vegetation characterization
20 (e.g. Verrelst et al., 2015). As the PALM model requires high spatial resolution for performing building-resolving simulations, the free and open Sentinel-2 satellite data is of interest as well as the data of commercial satellite constellations like Rapid Eye or World View. Additionally, false color airborne imagery, with its very high spatial resolution, would be preferable if available for the right time of year.

Especially in developed countries, public authorities and agencies routinely collect a vast amount of geo-spatial data sets.
25 The following focuses on the situation in Germany, because the selected study areas for the model development are located here. In Germany, available official data is hosted at different levels of agencies and departments (municipal, federal state, state, cadastral office, etc.). The accessibility of the data differs between the federal states and municipalities. In some federal states, such as Berlin, Hamburg, Thuringa or North-Rhine-Westfalia the data is easily accessible and downloadable and available through the Open Data Licence. These data sets are also regularly updated. The possibility to use additional official data
30 depends on the purpose and costs. Municipalities interested in the resulting micro-climate simulations usually provide their data on request for the purpose of a scientific study. The various German official data sets which are useful and available for most municipalities are shortly addressed below. The cadastral data of ATKIS and/or ALKIS (Working Committee of the Surveying Authorities of the States of the Federal Republic of Germany, 2015) are used for the estimation of the building age when no detailed information on individual buildings is available. Additionally, the data can be used for the localization of



streets, public open spaces and water bodies. ATKIS and ALKIS are regularly updated every one to three years (depending on the land use category). The municipal parks and open spaces departments host the data of the public green spaces and tree register. The latter is usually only available for trees on public ground. Information about trees and green spaces on private property have to be derived from additional data sources. If a tree register is available it provides comprehensive information

5 on tree species, age, height, and sometimes also crown and stem diameter. Building data is provided in form of 3D building models in level of detail LOD1 (block buildings without exact roofs) or LOD2 (more detailed with roof parts). Whereas LOD1 data sets are available for entire Germany, LOD 2 data is currently only available for some federal states. Nevertheless, a German-wide coverage is planned for the end of 2019 (Arbeitsgemeinschaft der Vermessungsverwaltungen der Länder der Bundesrepublik Deutschland, a, b). A standardized data format for 3D city models is City Geography Markup Language

10 (CityGML, Open Geospatial Consortium (2012)), an XML based data format that can be used to describe the city in 3D at different levels of detail. Digital terrain, surface models or LiDAR data as well as aerial images are available at the departments of geo-information or land survey administration at the federal state level in general. Aerial images are updated in a 2 to 5 years period to monitor the green volume development. For this purpose the images have to include the near infrared band. The acquisition dates differ - dependent on their primary purpose- from early spring to summer and thus have a minimal or dense

15 broad leaf cover. Only the summer images present the phenological state needed to detect the tree canopy and with that the leaf area index (LAI) and leaf area density (LAD). Soil data is available at the municipal level or at the state level in different scales from 1:10,000 till 1:200,000. The municipal data cannot provide the full information for a model parameterization, so that additional data acquisitions and/or data fusion is needed.

Surprisingly, municipalities – at least in Germany – usually don't systematically collect spatially detailed information on

20 the road network and pavement types. This gap can be closed using Volunteered Geographical Information from the Open-StreetMap (OSM) project. One caveat of such crowd driven data collection is that anybody can add any features and tags they think relevant, so no homogeneous data quality, completeness and adherence to a single standard can be guaranteed (Quinn and Bull, 2019). However Haklay (2010) and Graser et al. (2015) show that at least in western Europe OSM has a data quality en par with governmental sources. OSM can be utilized to add missing information to the government data e.g., about road type,

25 pavement type, bridges, pedestrian crossing points, and water bodies.

Geodata can be stored in raster format, with a value for each raster cell or pixel. GeoTIFF is a common format supported by all geo-processing software, but also the NetCDF supports geo-spatial information. Spatial data in vector format uses the locations of point, lines and polygons with optionally attached attribute tables containing additional information on each spatial object. A commonly used vector format is the ESRI Shapefile. Governmental data are often in vector format, as there are many

30 attributes that describe an object. Remote sensing data are mainly raster data, as such data is recorded by the sensor in a regular grid.



4 Pre-processing of input data

This section introduces an exemplary strategy and workflow for the selection and pre-processing of the input data sources for PALM 6.0. This is demonstrated for three cities in Germany with varying availability of input data: Berlin, Stuttgart and Hamburg. Despite the variety of data sources, it was aimed to automate the pre-processing for each layer as much as possible to ensure replicability and to handle the vast volume of data (0.5 – 1 TB per city, depending on target resolution and city area). This resulted in a collection of pre-processing scripts to which adaptations have been made for each of the three cities.

The municipal data of Berlin including the aerial imagery and 3D city model was retrieved from the Berlin Geoportal FIS Broker³. The municipal data including the aerial imagery and 3D city model Hamburg was retrieved from the Transparenzportal of the governmental offices in Hamburg⁴. The municipal data including the aerial imagery and 3D city model of Stuttgart was provided by the Landeshauptstadt Stuttgart for use in the [UC]² project (Scherer et al., 2019). Other sources of data are indicated directly in the text.

4.1 Terrain height

Active remote sensing systems are valuable sources to generate digital surface models. For the layers of Berlin, Stuttgart and Hamburg, products of two different active sensors are combined. Within the municipality boundaries, the terrain height is directly retrieved from the 3D city model's LOD0 data derived from airborne LiDAR data as provided by each of the municipalities^{5 6}. As this data set ends at the municipal boundaries, a satellite based, yet coarser data set is added to provide terrain height for the surrounding areas, as PALM always requires a rectangular area. In this case, the 30 m SRTM digital elevation model (DEM) was used. It is derived from the Shuttle Radar Topography Mission (SRTM) (Farr et al., 2007). For Stuttgart and Hamburg, the SRTM data set first had to be transformed from the global lat/lon geoid to the local German geoid. Subsequently, the SRTM DEM was clipped and resampled to the study areas with 1 m spatial resolution. Finally, the local terrain model and the SRTM terrain model were merged, with the local terrain model as primary source. A feathering distance of 100 pixels was assigned for borders of the local terrain model to smooth any abrupt changes in height between the two data sets. The final terrain height data set for each of the three cities is shown in Fig. 1.

4.2 Surface classification

PALM differentiates between building and land surface grid cells, where the land surface grid cells must consist of vegetation, pavements or water bodies (see Sect. 2.4). The first task within the surface classification is to map these four classes (buildings, vegetation, pavements and water bodies). In the sections below it is described how the according maps are prepared so that they can be written out into the static driver file. As soon as they are available, possible gaps, which usually result from combining data sets of different sources or as result of rasterization, need to be filled, in at least one of the core classes (see Sect. 2.1).

³<https://fbinter.stadt-berlin.de/fb/index.jsp>

⁴<http://transparenz.hamburg.de/das-transparenzportal/>

⁵Berlin: https://fbinter.stadt-berlin.de/fb/feed/senstadt/a_dgm

⁶Hamburg: <http://suche.transparenz.hamburg.de/dataset/digitales-hohenmodell-hamburg-dgm-16>

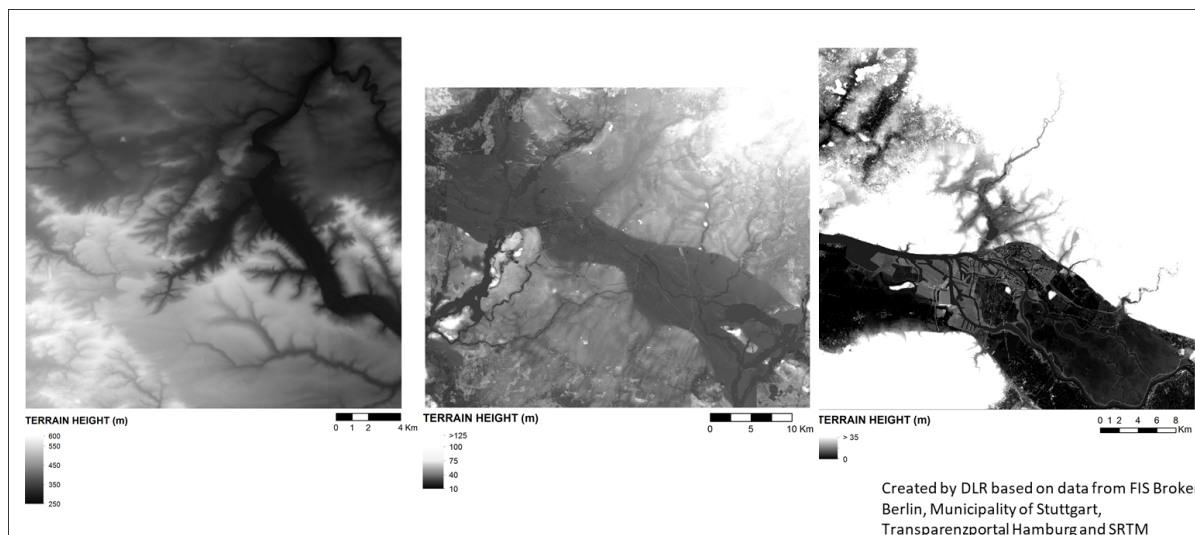


Figure 1. Terrain height for the study areas in m above ground. From left to right: Stuttgart, Berlin and Hamburg.

To achieve this, the layers were ranked according to their spatial reliability, e.g, the building layer was preferred over the – often courser – vegetation layer. Secondly, extra secondary buffered input layers were generated where possible and used to fill in their primary layer for pixels where none of the primary layers or prior filled layers had valid data. For example this was necessary for roads, where exact information on roadside parking was not available and thus the actual paved surface is wider than what would be expected from the road width. If there were still holes after all the filling iterations they were filled with a prevalent reasonable value like bare soil.

After the general surface classification is done, unique IDs for each of the buildings and bridges are generated to mark which pixels belong to the same object to support processing in PALM (see Sect. 5.2).

4.3 Buildings

10 For all the cities the building height, building type and building IDs were derived.

4.3.1 Building height

For realistic simulation results of both the flow and the thermodynamic interaction with the urban canopy, it is essential to have the spatially resolved and correct building height. In Germany municipalities have 3D building outlines in LOD1 (block model) or LOD2, which contains differentiated roof structures and therefore allows spatially explicit height calculation for each pixel. For Hamburg and Berlin LOD2 data was available as CityGML (Open Geospatial Consortium, 2012) data⁷⁸, while in Stuttgart LOD2 building height data was provided as 3D triangulated irregular network (TIN). The developed approach to

⁷Berlin: https://fbinter.stadt-berlin.de/fb/feed/senstadt/a_lod2

⁸Hamburg: <http://suche.transparenz.hamburg.de/dataset/3d-stadtmodell-lod2-de-hamburg4?forceWeb=true>



calculate the building height is a two step approach. In a first step the 2D-coordinates of all pixel centroids inside a single polygon as well as the 3D-bounding box of the polygon is calculated using the algorithm from the GDAL Library GDAL/OGR contributors (2019), which can cope with complex building geometries including inner courtyards etc. If the polygon is of single height, which is (nearly) always the case for floor polygons, this single height is used for all pixels. For each single centroid-coordinate the 3D intersection between its vertical line and the plane of the polygon is calculated to get the height of the building at this position. The special cases that the vertical line is inside or parallel to the plane (building walls directly passing through pixel centroids) are filtered. The calculated height values are capped to the z -range of the bounding box. This is necessary to compensate for rounding errors in nearly vertical planes, which could lead to single intersects wrongly being near infinite. The minimal and maximal height intersection is stored for each pixel. This approach works on the assumption that all the single polygons are planar polygons as defined in the cityGML standard (Open Geospatial Consortium, 2012), where all points of a polygon are in the same plane. However, for some single buildings in Berlin this assumption proved wrong as roof planes included single points from the walls of floors. These polygon errors were corrected where possible and otherwise removed from further calculations. Once all polygons have been processed the building height is calculated as the difference between max and min intersection. In a second iteration the same approach is repeated for all pixels that intersect the boundary of the polygons, but where the centroid is outside the polygon. However, these height values are only used for pixels where no building height was calculated in the first iteration. This two step approach guarantees that the extrapolation (with capping at the z -range of the polygon) to coordinates outside the building footprint is only performed if no other polygons contains the centroid of this pixel. Therefore a higher building which slightly intersect the corner of a pixel will not interfere with lower buildings that cover the pixel, while still removing a lot of single pixel holes with the other base layers (water, vegetation, pavement) This approach worked well for the city of Hamburg and Berlin, where some broken polygons had to be fixed beforehand. However in Stuttgart not all buildings had a closed floor polygon. Therefore in this case the terrain height was used as the lower boundary of the buildings. An example of the building height from the CityGML data of Berlin is given in Fig. 2 for the Reichstag building.

4.3.2 Building type

The building type used in PALM is defined through a combination of building use and the age of the building (see A2). In Germany, the municipalities often maintain a building use data base, e.g., in the ALKIS data sets. Usually this data is provided at building block level and therefore often contains mixed uses. For Stuttgart and Hamburg this data set was used to distinguish between residential and other building use⁹. The lookup table is given in Table B8. The cities of Hamburg and Stuttgart additionally maintain a data base documenting the age of the building. This allowed to assign the building type with quite high reliability. For Berlin, a combined data set is available, where building blocks are categorised by use and building construction period at the same time¹⁰. The look-up table to translate this information to building types is listed in Table B7. The building type maps for Stuttgart, Berlin and Hamburg are presented in Fig. 3. Note, however, that in Germany there is no cadastral

⁹Hamburg: <http://suche.transparenz.hamburg.de/dataset/alkis-ausgewahlte-daten-hamburg6?forceWeb=true>

¹⁰https://fbinter.stadt-berlin.de/fb/wfs/geometry/senstadt/re_isu5

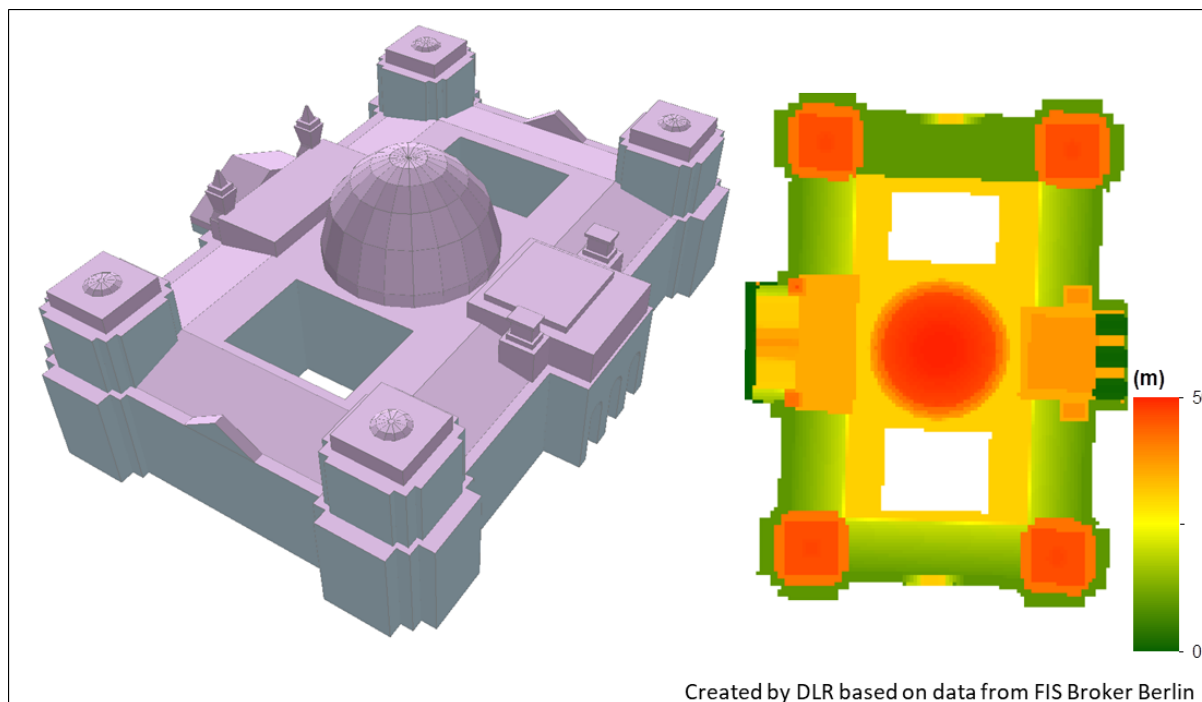


Figure 2. 3D visualisation of the CityGML data of the Reichstag building in Berlin (left) and the derived building height (right).

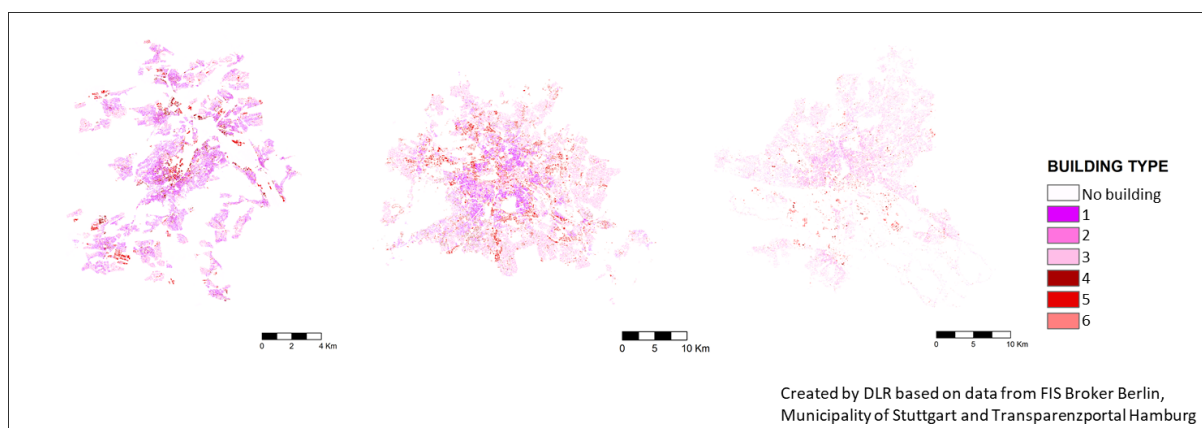


Figure 3. Building type maps of Stuttgart, Berlin and Hamburg (from left to right).

information on restoration and heat insulation actions for individual buildings, so that the age of building construction used for building classification is often a rather poor proxy for the thermodynamic properties of buildings.

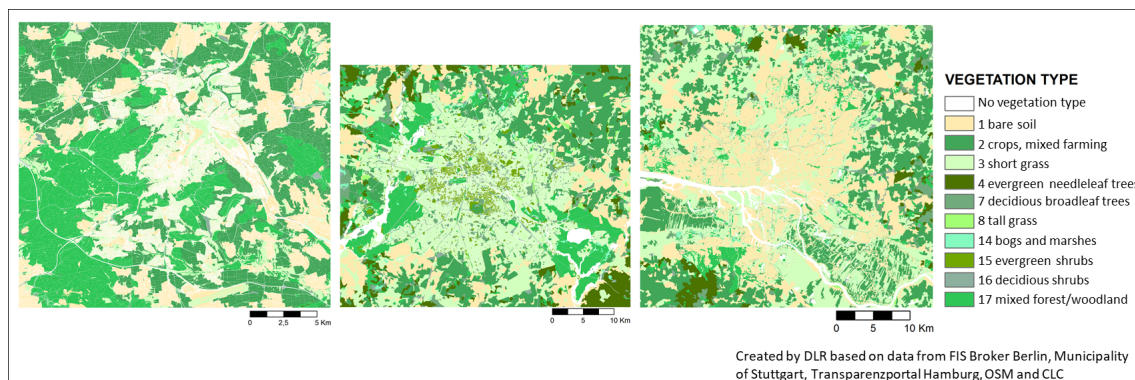


Figure 4. Vegetation type. From left to right: Stuttgart, Berlin and Hamburg.

4.4 Vegetation

PALM can handle very detailed information on the vegetation, as outlined in Sect. 2.6.1. In this study, the vegetation type was determined as well as vegetation on roofs and several characteristics of trees. As an area wide approach satellite or airborne imagery provides accurate information on the location of the vegetation as well as some vegetation characteristics, but not all.

- 5 Luckily, in Germany there is a huge amount of information available from municipal data that cannot be retrieved with remote sensing data alone. Also, open data such as OSM and other citizen science projects can provide valuable information on the urban vegetation. Therefore these sources are all combined to derive as complete input data for PALM as possible.

4.4.1 Vegetation type

For the vegetation type layer municipal data was used in the three demo-cities, including ALKIS (Berlin) and the Biotope Cadastre (Hamburg). For Stuttgart, such municipal data was not available, thus OSM was used as a main source here. Subsequently, gaps were filled with data from Corine Land Cover (CLC, European Union (2017)), which was especially the case for the areas outside the municipal borders. Missing data and gaps in the layer between vegetation and other features are filled up using aerial color and infrared images (CIR images), using a threshold on the NDVI to differentiate between grass and trees. For the different data sources lookup tables have been created to map the classes of OSM¹¹ (Table B2), CLC (Table B2) and the biotope maps of Hamburg¹² (Table B3) to the vegetation types of PALM. The main classes of ALKIS already directly match the PALM vegetation types. The vegetation type layer was created together with other layers as described in Sect. 4.2. As a result, the vegetation type layer is empty in locations of streets and water bodies. The result is shown in Fig. 4.

¹¹<https://planet.openstreetmap.org/>

¹²<http://suche.transparenz.hamburg.de/dataset/biotopkataster-hamburg1?forceWeb=true>



4.4.2 Vegetation on roofs

Intensive and extensive green roofs are detected using municipal 10 to 20 cm Ortho near infrared (CIR) images in combination with the building footprints for the cities of Berlin and Stuttgart. The percentage of green roof vegetation is aggregated for each building roof Pixel. The mostly very extensive green vegetation on roofs is detected by analysing the Normalized Difference

5 Vegetation Index (Rouse et al., 1974):

$$NDVI = \frac{\rho_{nir} - \rho_{red}}{\rho_{nir} + \rho_{red}} \quad (1)$$

where ρ_{nir} is the reflection in near infrared part of the spectrum and ρ_{red} the reflection in the red part of the spectrum. The NDVI utilizes the unique characteristic of photosynthetic active vegetation to absorb light in the red part of the spectrum and emit it in the near infrared, making vegetation distinguishable from other materials. Minimum and maximum thresholds on the NDVI were determined empirically from the aerial images, as the thresholds depend on the vegetation conditions during image acquisition, the pre-processing and colour enhancing steps during the creation of the images as well as the sensor-systems used aboard the plane. Therefore the thresholds vary between cities. The lower threshold (0.2 in Berlin, 0.06 in Stuttgart) distinguishes the extensive vegetation from bare roofs, while the upper bound (Berlin 0.4 ,Stuttgart 0.25) is used to distinguish extensive from intensive vegetation and remove these from the green roof vegetation. The strong vegetation signal is mostly caused by trees growing over the roof, rather than on the roof or by potted plants. Figure 5 also shows the problems associated with merging information from different sources, as the aerial images do not fully compensate for the perspective of oblique sideways acquisition -especially for higher buildings- there is a shift between the building outline and where it is recorded in the image. This can lead to erroneous vegetation along the borders of buildings, both over and underestimating the vegetation. In Hamburg no near infrared aerial data was available at the time to create the green roof layer.

20 4.4.3 Trees

To resolve tall vegetation (i.e., trees), a range of additional parameters have to be specified that support the generation of leaf area density (see Sect. 5.3). In this study, we aimed at deriving tree height, crown diameter, trunk diameter, tree type and tree species, as well as leaf area density, which is described in Sect. 4.4.5. While tree height and crown diameter could be derived from LiDAR data (Fassnacht et al., 2016), the other parameters are very difficult to acquire without extensive field surveys. Luckily, many German cities have so called tree cadastres, where they store exactly these characteristics to support the maintenance of public trees. Such data sets were available for Berlin, Hamburg and Stuttgart, although the Stuttgart data set only included tree species. Please note that in these municipal data sets only public trees (e.g., along public roads) are included. Private trees, e.g., in gardens and public parks are missing. If no additional sources are available (e.g., as described in Sect. 4.4.4, this means that the uncertainty increases of representing real-world conditions in PALM.

30 To prepare the data for PALM, look-up tables for tree type and species were created, which contain all species and types of trees recorded in the three cities. A class number was assigned to each type and species and then joined to the attribute table of the tree cadastre Shapefile. Varying spellings for the same type or species were taken into account and assigned the same

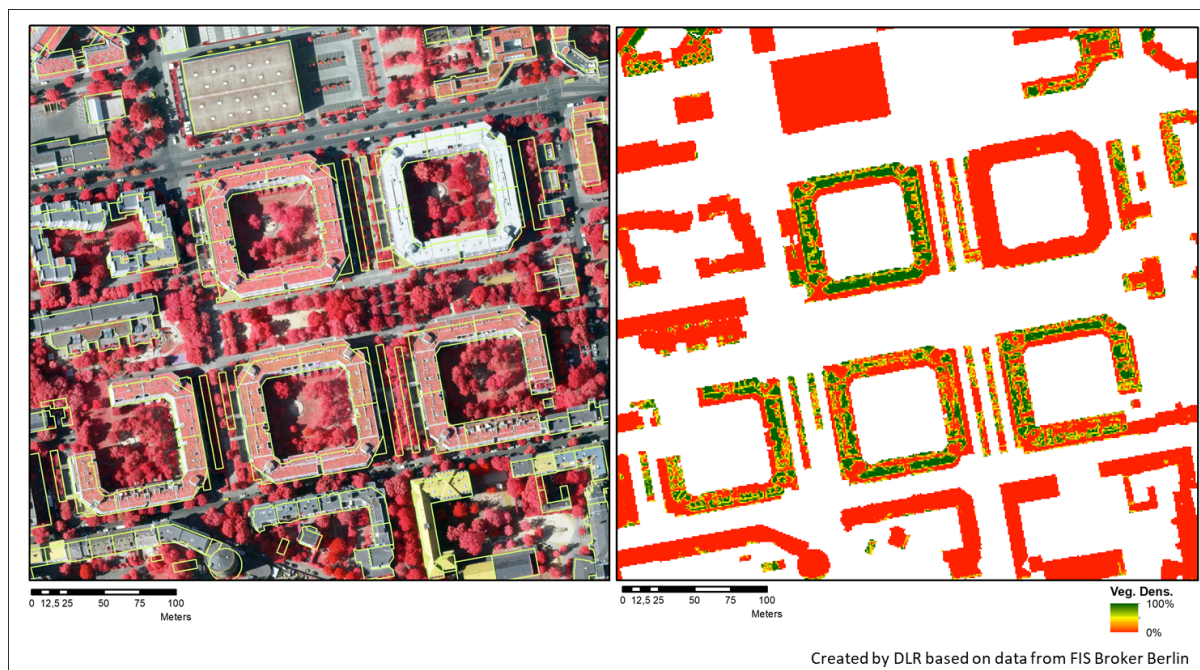


Figure 5. 10cm CIR image of a small subset of Berlin on the left, overlaid with the building outlines in yellow. The perspective offset between the orthoimage and the building outlines is especially pronounced for the high round building at the bottom. The resulting vegetation density Map for PALM at 1m resolution is shown in the right illustration.

value. For the attributes age, height, trunk diameter and crown size all numbers were checked for plausibility and corrected if obviously wrong (typos, wrong unit). The resulting Shapefiles were converted to raster (geoTIFF) and then NetCDF. Fig. 6 shows exemplary tree type and age maps for a subset of Berlin.

4.4.4 Vegetation patch

- 5 Instead of providing tree properties of single trees, it is also possible to provide the information on the high vegetation in an area wide manner, as vegetation patches. This is practical, as the tree data sets that were available only cover the public trees. Information on all other trees need to come from another source. Suitable sources are LiDAR data or to some extent also (governmental) forestry data. Not all cities in Germany have LiDAR data sets, but for Berlin we could use a LiDAR based data set as well as forestry data. The city of Berlin provided a vegetation height map¹³, that included the height for all
- 10 vegetated areas, thus including both public and private trees and shrubs as well as vegetation in parks. For forest vegetation outside Berlin, the Umweltatlas of Berlin (Environmental Atlas) provided information on average tree height, age, type and trunk diameter at breast height for each forest lot as a Shapefile¹⁴. The LiDAR based vegetation height and the vegetation

¹³<http://www.stadtentwicklung.berlin.de/umwelt/umweltatlas/i509.htm>

¹⁴<http://www.stadtentwicklung.berlin.de/umwelt/umweltatlas/ib504.htm>

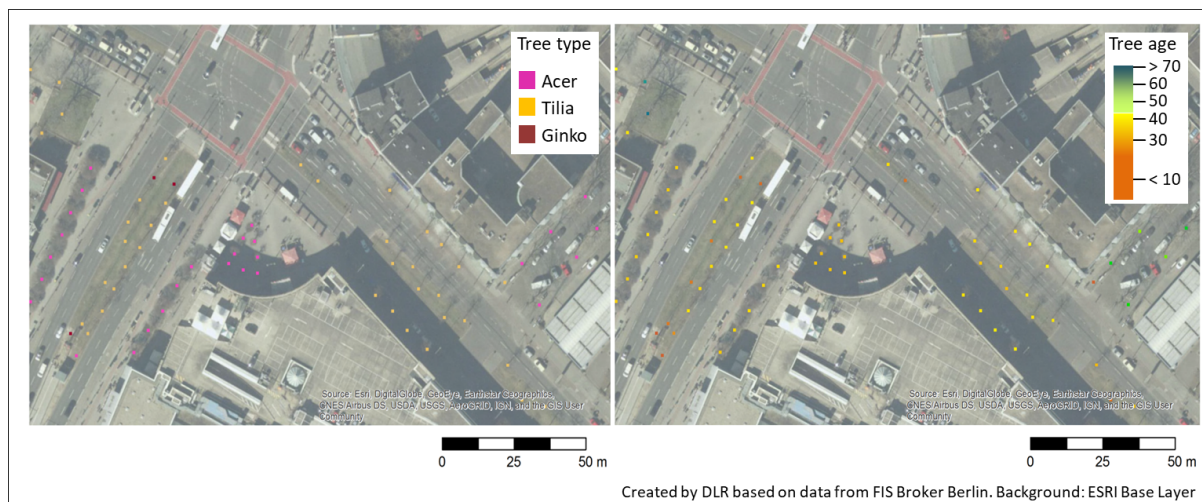


Figure 6. Tree species (left) and tree age (right) of municipal trees in Berlin

height of the Umweltaltas were merged, using the LiDAR based vegetation height as primary data set. The resulting map for the vegetation patch height is shown in Fig.7.

4.4.5 Leaf area index

The LAI is an important parameter for the generation of the LAD, which is described in Sect. 5.3. As the LAI varies largely over the phenological cycle, remote sensing is the most suitable data source. Field measurements on the ground only sample single trees, but with area wide remote sensing data an estimation of the LAI of larger area is possible. Typical approaches for LAI estimation make use of vegetation indices in combination with empirical relationships between a vegetation index and LAI. As only multispectral remote sensing imagery was available for this study, an NDVI based method was selected, making use of Sentinel 2 optical satellite data. Depending on the study area up to three image granules had to be combined to create a complete coverage of the city area. This is only possible if cloud free granules of the same or close dates are available. The aim was to create cloud free coverages for each season. Using data of the year 2017, cloud free images of Berlin, Stuttgart and Hamburg could be created for spring and summer, as well as an additional winter image for Hamburg and an autumn image for Stuttgart.

Using the Timescan processing chain (Esch et al., 2018) the NDVI was derived for all Sentinel 2 scenes. For each date range, an NDVI mosaic image of the study area was created using GDAL tools (GDAL/OGR contributors, 2019). Then the LAI is calculated using an IDL algorithm for each study area and date. For this, an empirical relationship between NDVI and LAI is used as documented by Wang et al. (2005) for deciduous forest. All non-vegetation pixels are set to 0 (vegetation mask). As the spatial resolution of Sentinel 2 is 10 m, the required resolution of 1 m is reached by resampling the LAI map using a bilinear resampling method. For a subset of Hamburg the estimated LAI is presented in Fig.8 for three seasons.

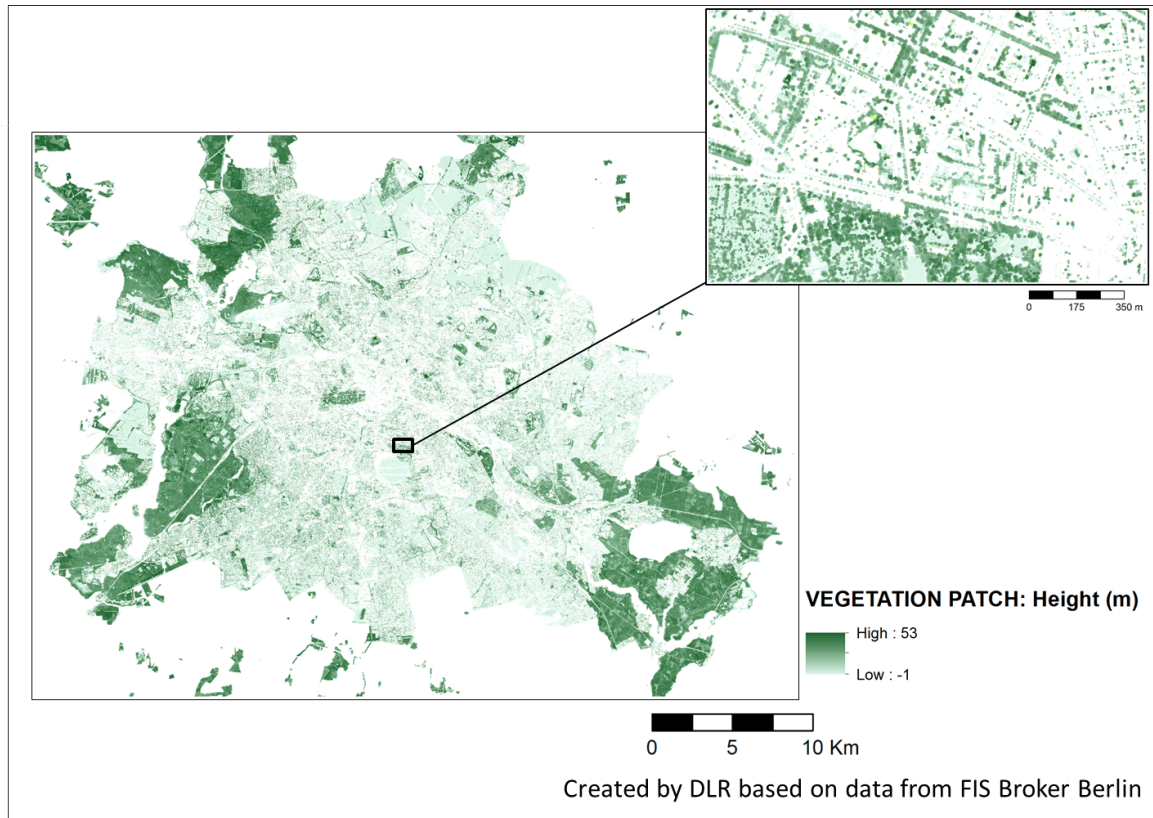


Figure 7. Height of vegetation patches in Berlin



Figure 8. LAI for a subset of Hamburg in winter (2-14-2017, left), spring (4-20-2017, center), and summer (8-23-2017, right)

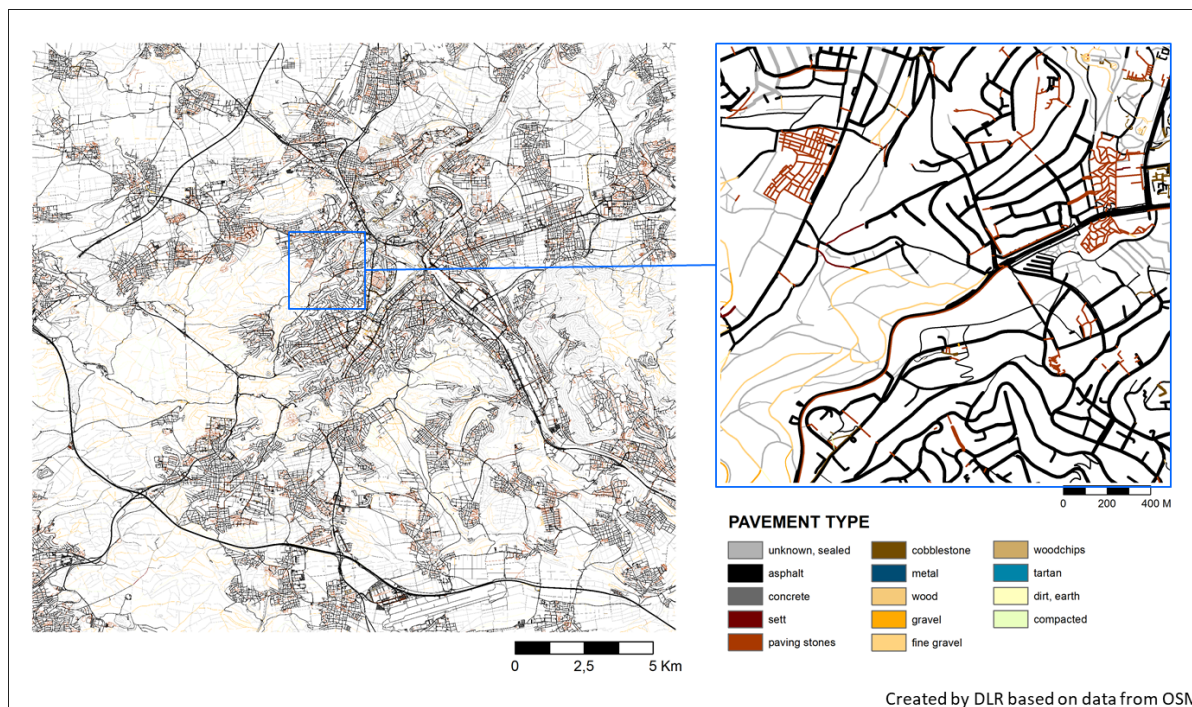


Figure 9. Pavement type of Stuttgart

4.5 Pavements

As a source for the pavement layer airborne hyperspectral would be very good. Such spatially and spectrally detailed data would allow a differentiated classification of urban surface materials (van der Linden et al., 2019; Roessner et al., 2001). However, due to its experimental nature, hyperspectral data is rarely available for whole cities. Therefore, OSM data was used instead. OSM contributors not only mapped road features, but often also indicated the surface materials. As the contributors do not apply homogeneous labels, a lookup table was created to map all the materials listed in OSM for the test cities to the PALM pavement types. If no surface material is indicated, default materials are assumed for each road type (Table B5). Using another look-up table, the materials were matched to the pavement types listed in the PIDS. As the roads in OSM are line features, each road is buffered with the width or, if not available, a default width for that type of road (Table B5 and B6). After rasterization, the data set is checked for gaps between pavement type, vegetation type, buildings and water. Gaps are filled with the road pavement type by applying a larger buffer (3 x the listed diameter) on the road lines. An example of the resulting pavement type raster map is shown in Fig. 9.

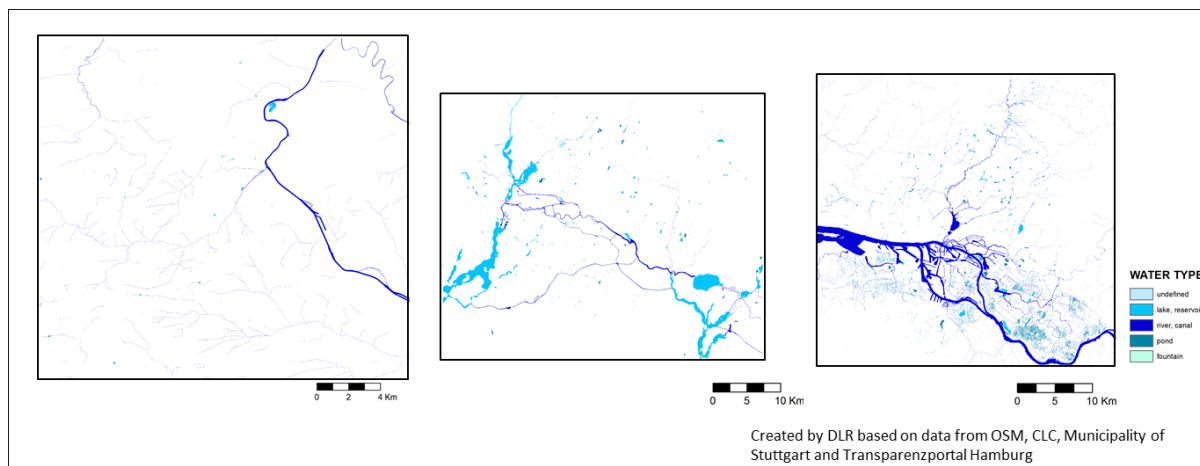


Figure 10. Water type of Stuttgart, Berlin and Hamburg (from left to right)

4.5.1 Street type and street crossings

For the street types and street crossings data from OSM is used. Street types directly use the classes specified in OSM and are assigned to the road grid cells. If multiple road types cover a pixel, the highest class is assigned. Thus a motorway would have precedence over a primary road ect. A street crossing flag is assigned to all parts of the streets that are marked in OSM as street crossing. As this label is a point feature, all grid cells in a buffer of 15 m around each crossing point are flagged as crossing.

4.6 Water bodies

Multispectral remote sensing is a suitable tool to map water bodies (Ma et al., 2019), but at the high spatial resolution required for building-resolving simulations, the spatial resolution of most satellite data is not sufficient. Also aerial images usually do not provide enough (and calibrated) spectral bands, to distinguish smaller water bodies like fountains or rivulets. Therefore, also in this case OSM was used as primary source for the demo-cities. Unfortunately, it turns out OSM is incomplete regarding water bodies. Therefore the data sets were merged with CLC data for Stuttgart and ALKIS and the Biotop Cataster in Hamburg. Look-up tables were created to assign a PALM water class to each water feature in the different data sets (see Table B9 and B11). ALKIS polygons are sorted into water types that match the PALM water types (Working Committee of the Surveying Authorities of the States of the Federal Republic of Germany, 2015). Also CLC contains classes that map directly to the PALM water types (European Union, 2017). After the data sets were merged, for Stuttgart and Berlin several important water bodies had to be added manually. The final water type maps for the cities of Stuttgart, Berlin and Hamburg are presented in Fig. 10.

4.7 Soils

As soil data is difficult to acquire, especially at resolutions less than 10 m, a horizontally and vertically homogeneous soil type distribution (with soil_type = 1, coarse soil texture) is assumed in this study, i.e. the physical properties of the soil are



identical all over the model domain. Further information on the initial state of the soil moisture and temperature at each pixel can be given as LOD0 via Fortran Namelist input, or as LOD1 input given in the dynamic input file (Maronga et al., 2019). The respective soil information can be e.g. take from mesoscale models such as COSMO or WRF, which will be described in a separate follow-up paper.

5 5 Preparation of input data for PALM

In this section we discuss PALM static driver generator, the generation of three-dimensional vegetation data in terms of LAD and basal area density (BAD) fields from two-dimensional information as part of the static driver, as well as the internal topography processing which is required to ensure all PALM requirements on the terrain data are met. Note that the netCDF interface routine in PALM has undergone several improvements since the official release of PALM 6.0. In the following, we will thus describe the status quo for PALM 6.0 in revision 4311.

5.1 Using the PALM static driver generator

In order to enable the user to create static drivers for complex scenarios, the Python 3.0-based pre-processing tool `palm_csd` (short for: PALM create static driver) is shipped with PALM. The tool comes with a comprehensive library with netCDF functions and utility routines that can also easily be plugged in into user-specific Python codes, and which take care of the correct formatting of static driver files that comply with PALM's netCDF interface. `palm_csd` itself, however is a wrapping and compiling tool, which compiles static drivers based on already processed and rastered geospatial data in netCDF format, but it cannot process other geospatial file formats (e.g., GeoTIFF or Shapefile). At the moment, it is thus up to the user to process such data manually and provide `palm_csd` with PIDS conform NetCDFs. Currently, input data for `palm_csd` is available for the cities of Berlin, Hamburg, and Stuttgart in Germany, for which input data was processed based on the data sources outlined in Sect. 4, but the user is free to provide his own data to be processed by `palm_csd`. Note that while data for Berlin and Hamburg is freely available for the general public, data of Stuttgart is restricted to be used within the [UC]² project. During the pre-processing of the data for Berlin, Hamburg and Stuttgart it was aimed to automate the pre-processing steps as much as possible by implementing the geo-processing in scripts and reduce manual processing in GIS software. In the next phase of [UC]² it is planned to develop a pre-processing tool that will support users to generate the input data in PALM conform formats.

`palm_csd` is steered via a configuration file in which input files, basic settings, and default values are defined. Once this configuration file is set-up, the user can generate his own static driver files that include correct metadata and possibly geo-referencing (depending on suitable input data) for PALM and that will also be written to PALM's output data for post-processing and visualization.

We plan to extent `palm_csd` for generic and academic setups as well as with a graphical user interface in near future. Moreover, we plan to implement a comprehensive checking routine so ensure compatibility with PALM, which is currently done within PALM itself.



5.2 Internal topography processing

During the initialization of PALM, the provided topography data, encompassing terrain height and buildings, is further processed and could be possibly slightly modified, e.g., to fulfill numerical requirements or to reduce the use of computational resources.

5 The model surface in PALM is internally defined at $z = 0$ m. Therefore, in a first step, PALM internally computes the relative terrain height $z'_t = z_t - z_{t,\min}$, where $z_{t,\min}$ is the minimum terrain height occurring within the model domain. Thus, the minimum z'_t coincides with the model surface at $z = 0$ m and the first vertical grid level has at least one grid point that lies within the atmosphere. For instance, if z_t is given in meters above sea level and we would use this without any further processing, many grid points may lie below the Earth surface, being a waste of computational resources without providing
10 any additional value. In case of a nested simulation setup with a root domain and various child domains, $z_{t,\min}$ is calculated as the minimum terrain height over all domains, in order to have the same reference height for all model domains and avoid artificially induced elevation changes at the domain borders between the parent and the child models.

In the following, $z'_t(y, x)$ is projected onto the discrete grid, while all grid points are flagged as terrain that are located below $z'_t(y, x)$, as illustrated in Fig. 11 by the dashed black line.

15 In a second step buildings are mapped on top of the discrete terrain, which is illustrated schematically in Fig. 11. Especially when the underlying terrain is not flat but elevation changes occur below a building, roof shapes should be maintained, so that buildings can't be simply mapped on top of z'_t . Hence, the underlying terrain below a single building (which is identified by its `building_id`) is padded up to the level of the highest $z'_t(y, x)$ within the building-covered area with respective `building_id`: $z'_t(y, x) = \max(z'_t(y, x))_{ID}$, i.e., the terrain below the building is flattened (please see the hashed areas in
20 Fig. 11). This guarantees that building and roof shapes are maintained even at steep slopes. However, an exception is made for bridges (identified by `building_type = 7`) where `buildings_3d` is directly mapped on top of z'_t . Flattening the terrain below the bridge to the highest terrain height (often the top of the levee) would otherwise introduce barrier-like topography structures.

While buildings are mapped onto the terrain, grid points that lie within buildings and below terrain are internally flagged,
25 in order to classify building- or land-surfaces during the surface initialization (see Sect. 2.4). The padded grid points below buildings will be not flagged as building but as land-surfaces, while these artificially introduced vertical land-surfaces will be initialized using the given `vegetation_type` or `pavement_type` at the adjacent grid cell.

After the topography is finally projected onto the discrete grid, it may contain single cavities or chimney-like holes that are only resolved by one grid point. Due to numerical issues, such one-grid-point cavities must be filtered. In many cases these
30 filtered cavities are building courtyards that are resolved by only one grid point. In this case, the courtyard grid point, which might be originally given, e.g., a `vegetation_type`, is internally flagged and re-set to a building grid point while it obtains `building_type`, `building_id` and, if available, `building_pars` from the nearby building grid point. Hence, we filter such one-grid point cavities during the model initialization, meaning that small differences might occur between the final building and terrain geometry in the model and the provided one in the static driver.

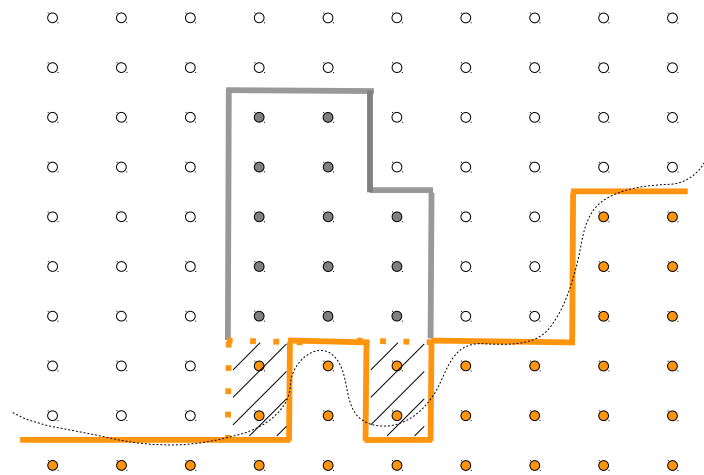


Figure 11. Schematic illustration on how buildings are mapped onto the underlying terrain. The thin dashed black line indicates the original relative terrain height z'_t . Solid orange lines indicate the original discrete terrain surface, while dashed orange lines indicate the resulting discrete terrain surface after the terrain is flattened below buildings, as indicated by the hashed areas. Grey solid lines indicate building surfaces. Orange and grey coloured points indicate terrain and building grid points, respectively, while non-filled points indicate atmospheric grid points.

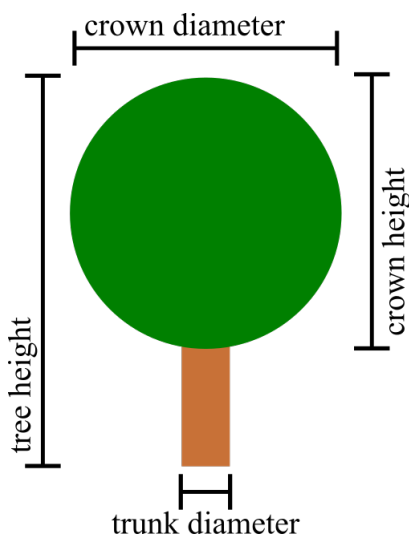


Figure 12. Schematic view of the parameters for a spherical tree shape through which the three-dimensional structure of trees are constructed in the single-tree canopy generator.

5.3 Generation of three-dimensional leaf area density and basal area density fields

When using PALM at very high resolution in the order of 1 m, vegetation like tall shrubs or trees can not be represented by common parameterizations that assume the vegetation canopy to be flat and represented, e.g., by a roughness length. Under such conditions, PALM employs a plant canopy model in which high vegetation can be represented in terms of three-dimensional LAD fields. As geospatial data usually does not yield any three-dimensional information, three-dimensional LAD and BAD fields must be estimated from two-dimensional data and other data sources. In order to allow for a pseudo-automated generation of LAD and BAD fields, `pal_m_csd` comes with two different routines for creating vegetation canopies: A routine for single trees as often found in urban environments, and a routine for creating vegetation canopies like forests and parks. In the following we will outline the basics of both routines. Note, however, that both routines are still in experimental stage and will be further developed and evaluated in the near future. In the following we will thus describe the status quo of these routines.

5.3.1 Generation of leaf area density and basal area density fields for single trees

Single trees, whose growth are seldom affected by other trees or obstacles can be characterized in terms of three-dimensional LAD and BAD fields by a limited number of parameters. In `pal_m_csd` these are the maximum tree height, crown diameter, crown shape, trunk diameter, height of the maximum LAD value, and the aspect ratio of tree crown diameter to tree crown height (see Figs. 12 and 13). In German cities, several of these parameters are available from tree cadastral register data. For example, for Berlin more than 400 000 municipal trees are collected in a publicly available database including information about tree species, tree height, crown diameter, stand age, and trunk diameter.

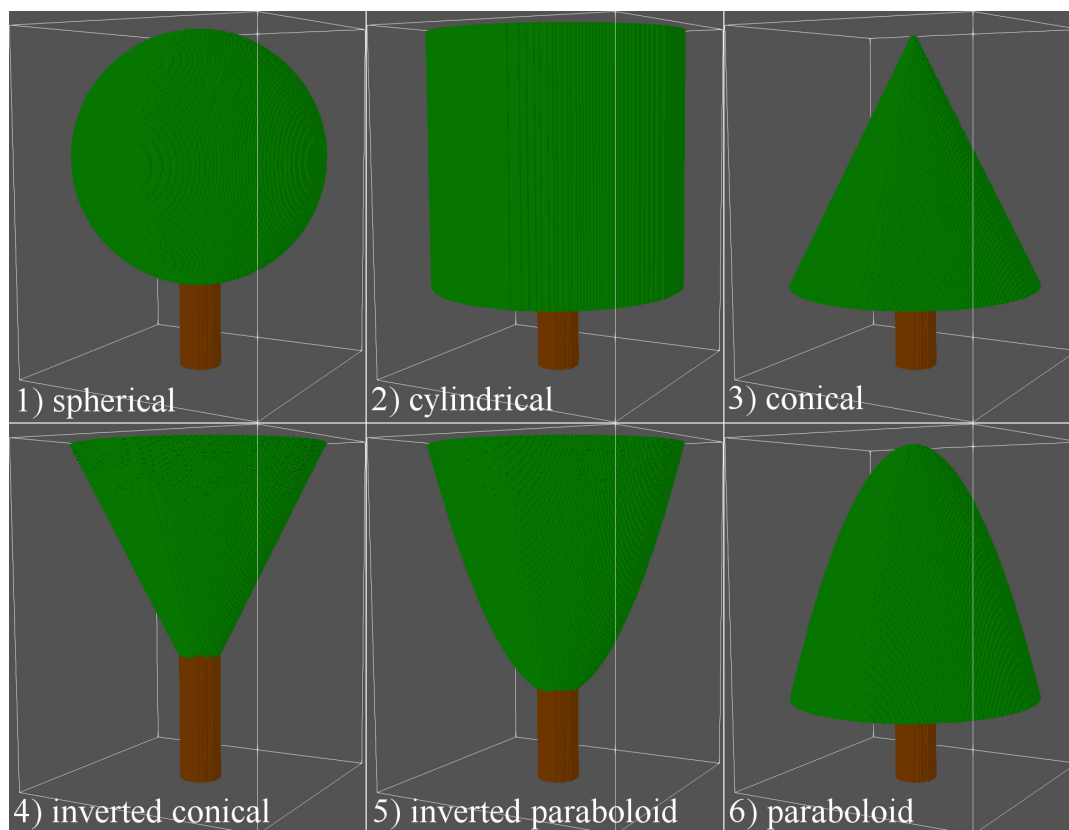


Figure 13. Overview of tree shapes available in the single-tree canopy generator. Green surfaces represent the foliage while brown surfaces represent the tree trunk. The shown sketches were created for a raster size of 0.05 m using a tree height of 8 m, a crown width of 6 m, a crown height to width ratio of 1, and a trunk diameter of 1 m.

The single-tree canopy generator in `palm_csd` is called for each individual tree and the following information is passed to the generator: location (y, x) of the tree centre, tree type (i.e., genus), tree height, LAI, crown diameter, and trunk diameter at breast height. If one or more of these parameters is not provided, a default value from a look-up table (see Table 16) is used, which was generated based on averaging each tree parameter for each tree type in the Berlin tree database. This look-up table also includes default values for the tree shape, the ratio between crown height to crown width, LAI values for summer and winter time, and the height of the LAD maximum. Note for some of the latter parameters only dummy values are currently available (crown height to width ratio, LAI, height of LAD maximum) and more effort will be needed to fill this table with reasonable data. The tree generator allows for six different tree shapes which are shown in Fig. 13 and which cover most of the commonly observed shapes for single trees. The generation of a three-dimensional LAD volume then consists of two steps. First, the volume covered with leaves is determined based on the shape, crown diameter, tree height, and the ratio of crown height to width. Second, the three-dimensional LAD field is created using an exponentially increasing LAD towards the

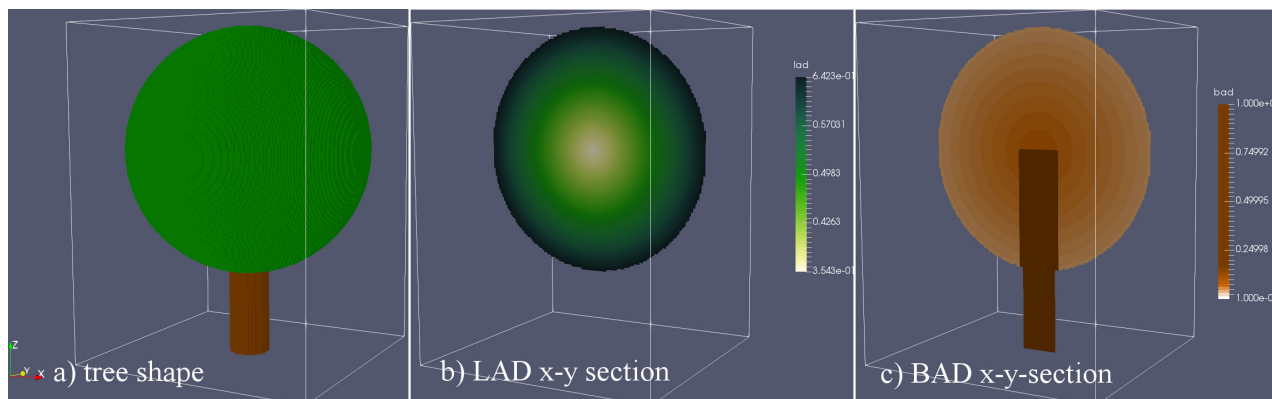


Figure 14. Exemplary distribution of LAD and BAD fields for a spherical-shaped tree. Shown are (a) the three-dimensional tree surface and $x - y$ -sections of (b) LAD and (c) BAD through the center of the tree.

outer shell of the foliage. This approach is based on the empirical finding that sun light is absorbed when entering the foliage resulting in decreasing production of leaves.

Calculation of three-dimensional BAD fields is available using an interim solution, where the BAD field is calculated from the given trunk diameter, which is taken as constant up to the center of the tree crown. At the moment, the canopy generator only allows to treat each grid volume as either (impermeable) stem or no stem. The representation of grid volumes partially covered by trunks is thus not possible at the moment. BAD values within the crown canopy is calculated as

$$BAD = 0.1 \cdot (1 - LAD), \quad (2)$$

which reflects increasing BAD towards the center of the crown. An example of both lad and bad fields for an idealized spherical-shaped tree is shown in Fig. 14. Note, however, that PALM currently only supports LAD so that only the foliage is read from the static driver. The import of BAD data will be realized in near future.

5.3.2 Generation of leaf area density fields for tree stands

In many cases, information on individual trees is not available or tree stands (e.g., forests) have to be represented as a three-dimensional canopy. This is commonly realized by treating each column (y, x) separately and using normalized LAD profiles that are representative for homogeneous canopies. In `palm_csd` the method of Markkanen et al. (2003) based on a vertical LAD distribution that is derived from a given LAI field as well as two parameters α and β , which can be varied by the user to represent different types of tree stands. Additionally, a two-dimensional vegetation height field can be prescribed (if available) in order to take into account varying tree heights within the canopy stand. If information on LAI and vegetation height is not available, the user has to provide default values instead. Using this method it is possible to generate idealized vegetation canopies in terms of LAD fields, but it provides no means to derive BAD information. In the future we plan to use a similar method as described in Bohrer et al. (2007) to create BAD fields by synthetically localizing tree trunks.



6 Conclusions

In the previous sections, the input data requirements of PALM are described, it is demonstrated how this data can be prepared and what steps are carried out in `palm_csd` to set-up the static driver to have all input data ready for PALM. PALM comes with a framework that enables micro climate simulations for a real-world urban environment. Different levels of detail can be provided to PALM. If the model is run with interactive building- and land surfaces, a minimum of seven spatial parameters is required: soil type, building height, building id, building type, vegetation type, pavement type and water type. Each of these parameters can optionally be specified in more detail, based on available data. As it becomes clear from Sect. 3 and 4, a vast amount of data exist, but rarely exactly in the format required by urban micro climate models. Exemplary for this is the building type. The combination of building use and building age yields the PALM building types. However, it needs to be analysed if this is the most accurate representation of the energetic properties of the building, as the building age often doesn't include any information on renovation and modernisation of the building which have a huge effect on the energetic properties of a building. Selecting and acquiring suitable data sets is a major task, that should be weighted against the available resources to pre-process the input data and the desired detail of the PALM simulations. Additionally, the varying quality of different data sources result in different uncertainties of the input parameters. There are uncertainties resulting from the spatial resolution (e.g., the ability to distinguish small objects), but there can also be mapping or labeling errors and omissions. How these uncertainties propagate into the simulation results needs to be investigated in more detail. To support users in the decision, which parameter are worth the effort of acquiring and preparing more detailed information, sensitivity analyses of the input datasets are planned.

As the pre-processing of the input data is tedious, it is aimed to develop a processing chain that support users in formatting their GIS data (e.g., Shapefiles, geoTIFF, WFS ect.) into a NetCDF file following the requirements of PALM. To support model users in their data acquisition, a data base with freely available geospatial data for the mandatory set of parameters of PALM is aimed at. This will provide users a starting point for running PALM simulations. The primarily target will be Germany but also Europe wide or global data can be included, as far as the data sources allow this.

7 Code availability

The PALM model system is distributed under the GNU General Public License v3 (<http://www.gnu.org/copyleft/gpl.html>). The model source, documentation, user manual, and online tutorial are freely-available and can be downloaded from <http://palm-model.org>. The pre-processing tool `palm_csd` to prepare and create a PALM Static driver is shipped with PALM and is available under <https://doi.org/10.25835/0041607>.

8 Data availability

In the supplements, a sample static driver is available for a small area in Berlin near Ernst-Reuter Platz, Germany, with 1 m spatial resolution. The static driver is prepared for a winter scenario with leafless deciduous trees. The model domain is $256 \times 256 \text{ m}^2$ in the horizontal directions.

<https://doi.org/10.5194/gmd-2019-355>
Preprint. Discussion started: 4 May 2020
© Author(s) 2020. CC BY 4.0 License.



Appendix A: Palm Input Data Standard (PIDS) tables



Table A1. Land use classification parameters according to `vegetation_type` based on the IFS model classification. Note that the land use class 13 (ice caps and glaciers) has not been implemented yet.

Description	Class	$r_{c,min}$ s m ⁻¹	LAI m ² m ⁻²	c_{veg}	gD hPa ⁻¹	z_0 m	$z_{0,h}$ m	Λ_s W m ⁻² K ⁻¹	Λ_u W m ⁻² K ⁻¹	$f_{sw,in}$	albedo_type	ϵ
bare soil	1	0	0.0	0.0	0.0	0.005	$0.5 \cdot 10^{-4}$	0.0	0.0	0.0	17	0.94
crops, mixed farming	2	180	3.0	1.0	0.0	0.1	$1.0 \cdot 10^{-4}$	10.0	10.0	0.05	2	0.95
short grass	3	110	2.0	1.0	0.0	0.03	$0.3 \cdot 10^{-4}$	10.0	10.0	0.05	2	0.95
evergreen needleleaf trees	4	500	5.0	1.0	0.03	2.0	2.0	20.0	15.0	0.03	5	0.97
deciduous needleleaf trees	5	500	5.0	1.0	0.03	2.0	2.0	20.0	15.0	0.03	6	0.97
evergreen broadleaf trees	6	175	5.0	1.0	0.03	2.0	2.0	20.0	15.0	0.03	8	0.97
deciduous broadleaf trees	7	240	6.0	0.99	0.13	2.0	2.0	20.0	15.0	0.03	9	0.97
tall grass	8	100	2.0	0.7	0.0	0.47	$0.47 \cdot 10^{-2}$	10.0	10.0	0.05	8	0.97
desert	9	250	0.05	0.0	0.0	0.013	$0.013 \cdot 10^{-2}$	15.0	15.0	0.0	3	0.94
tundra	10	80	1.0	0.5	0.0	0.034	$0.034 \cdot 10^{-2}$	10.0	10.0	0.05	11	0.97
irrigated crops	11	180	3.0	1.0	0.0	0.5	$0.5 \cdot 10^{-2}$	10.0	10.0	0.05	13	0.97
semidesert	12	150	0.5	0.1	0.0	0.17	$0.17 \cdot 10^{-2}$	10.0	10.0	0.05	2	0.97
ice caps and glaciers (*)	13	0	0.0	0.0	0.0	1.3E-3	$1.3E \cdot 10^{-4}$	58.0	58.0	0.00	14	0.97
bogs and marshes	14	240	4.0	0.6	0.0	0.83	$1.3 \cdot 10^{-4}$	10.0	10.0	0.05	4	0.97
evergreen shrubs	15	225	3.0	0.5	0.0	0.10	$0.1 \cdot 10^{-2}$	10.0	10.0	0.05	4	0.97
deciduous shrubs	16	225	1.5	0.5	0.0	0.25	$0.25 \cdot 10^{-2}$	10.0	10.0	0.05	4	0.97
mixed forest/woodland	17	250	5.0	1.0	0.03	2.0	2.0	20.0	15.0	0.03	7	0.97
interrupted forest	18	175	2.5	1.0	0.03	1.1	1.1	20.0	15.0	0.03	8	0.97



Table A2. Building classification parameters according to `building_type` based on building age and usage.

Description	Class	Year of construction	Use
R1	1	< 1951	residential
R2	2	1951 – 2000	residential
R3	3	> 2000	residential
O1	4	< 1951	office
O2	5	1951 – 2000	office
O3	6	> 2000	office

Table A3. Pavement classification parameters according to `pavement_type` based on OpenStreetMaps. Thermal conductivity and heat capacity settings of the sub-surface pavement layers are given in table S4. Underlined values are preliminary

Description	Class	z_0	$z_{0,h}$	ϵ	albedo_type
asphalt/concrete mix	1	$5.0 \cdot 10^{-2}$	$5.0 \cdot 10^{-4}$	0.97	18
asphalt (asphalt concrete)	2	$5.0 \cdot 10^{-2}$	$5.0 \cdot 10^{-4}$	0.94	19
concrete (Portland concrete)	3	<u>$1.0 \cdot 10^{-2}$</u>	<u>$1.0 \cdot 10^{-4}$</u>	0.98	20
sett	4	<u>$1.0 \cdot 10^{-2}$</u>	<u>$1.0 \cdot 10^{-4}$</u>	0.93	21
paving stones	5	<u>$1.0 \cdot 10^{-2}$</u>	<u>$1.0 \cdot 10^{-4}$</u>	0.97	22
cobblestone	6	<u>$1.0 \cdot 10^{-2}$</u>	<u>$1.0 \cdot 10^{-4}$</u>	0.97	23
metal	7	<u>$1.0 \cdot 10^{-2}$</u>	<u>$1.0 \cdot 10^{-4}$</u>	0.97	24
wood	8	<u>$1.0 \cdot 10^{-2}$</u>	<u>$1.0 \cdot 10^{-4}$</u>	0.94	25
gravel	9	<u>$1.0 \cdot 10^{-2}$</u>	<u>$1.0 \cdot 10^{-4}$</u>	0.98	26
fine gravel	10	<u>$1.0 \cdot 10^{-2}$</u>	<u>$1.0 \cdot 10^{-4}$</u>	0.93	27
pebblestone	11	<u>$1.0 \cdot 10^{-2}$</u>	<u>$1.0 \cdot 10^{-4}$</u>	0.97	28
woodchips	12	<u>$1.0 \cdot 10^{-2}$</u>	<u>$1.0 \cdot 10^{-4}$</u>	0.97	29
tartan (sports)	13	<u>$1.0 \cdot 10^{-2}$</u>	<u>$1.0 \cdot 10^{-4}$</u>	0.97	30
artificial turf (sports)	14	<u>$1.0 \cdot 10^{-2}$</u>	<u>$1.0 \cdot 10^{-4}$</u>	0.94	31
clay (sports)	15	<u>$1.0 \cdot 10^{-2}$</u>	<u>$1.0 \cdot 10^{-4}$</u>	0.98	32



Table A4. Thermal conductivity $\lambda_{T,i}$ (in $\text{W m}^{-1} \text{K}^{-1}$) and heat capacity $(\rho C)_i$ (in J K^{-1}) of sub-surface layer i according to pavement_type classification. The underlined values are preliminary

Class	$\lambda_{T,1}$	$\lambda_{T,2}$	$\lambda_{T,3}$	$\lambda_{T,4}$	$\lambda_{T,5}$	$\lambda_{T,6}$	$(\rho C)_1$	$(\rho C)_2$	$(\rho C)_3$	$(\rho C)_4$	$(\rho C)_5$	$(\rho C)_6$
1	0.75	0.75	0.75	0.75	0.75	0.75	<u>1.94·10⁶</u>	<u>1.94·10⁶</u>	<u>1.94·10⁶</u>	<u>1.94·10⁶</u>	<u>1.94·10⁶</u>	<u>1.94·10⁶</u>
2	0.75	0.75	0.75	0.75	0.75	0.75	<u>1.94·10⁶</u>	<u>1.94·10⁶</u>	<u>1.94·10⁶</u>	<u>1.94·10⁶</u>	<u>1.94·10⁶</u>	<u>1.94·10⁶</u>
3	0.89	0.89	0.89	0.89	0.89	0.89	<u>1.76·10⁶</u>	<u>1.76·10⁶</u>	<u>1.76·10⁶</u>	<u>1.76·10⁶</u>	<u>1.76·10⁶</u>	<u>1.76·10⁶</u>
4	1.00	1.00	1.00	1.00	1.00	1.00	<u>1.94·10⁶</u>	<u>1.94·10⁶</u>	<u>1.94·10⁶</u>	<u>1.94·10⁶</u>	<u>1.94·10⁶</u>	<u>1.94·10⁶</u>
5	1.00	1.00	1.00	1.00	1.00	1.00	<u>1.94·10⁶</u>	<u>1.94·10⁶</u>	<u>1.94·10⁶</u>	<u>1.94·10⁶</u>	<u>1.94·10⁶</u>	<u>1.94·10⁶</u>
6	1.00	1.00	1.00	1.00	1.00	1.00	<u>1.94·10⁶</u>	<u>1.94·10⁶</u>	<u>1.94·10⁶</u>	<u>1.94·10⁶</u>	<u>1.94·10⁶</u>	<u>1.94·10⁶</u>
7	1.00	1.00	1.00	1.00	1.00	1.00	<u>1.94·10⁶</u>	<u>1.94·10⁶</u>	<u>1.94·10⁶</u>	<u>1.94·10⁶</u>	<u>1.94·10⁶</u>	<u>1.94·10⁶</u>
8	0.7	0.7	0.7	0.7	0.7	0.7	<u>1.94·10⁶</u>	<u>1.94·10⁶</u>	<u>1.94·10⁶</u>	<u>1.94·10⁶</u>	<u>1.94·10⁶</u>	<u>1.94·10⁶</u>
9	1.00	1.00	1.00	1.00	1.00	1.00	<u>1.94·10⁶</u>	<u>1.94·10⁶</u>	<u>1.94·10⁶</u>	<u>1.94·10⁶</u>	<u>1.94·10⁶</u>	<u>1.94·10⁶</u>
10	1.00	1.00	1.00	1.00	1.00	1.00	<u>1.94·10⁶</u>	<u>1.94·10⁶</u>	<u>1.94·10⁶</u>	<u>1.94·10⁶</u>	<u>1.94·10⁶</u>	<u>1.94·10⁶</u>
11	1.00	1.00	1.00	1.00	1.00	1.00	<u>1.94·10⁶</u>	<u>1.94·10⁶</u>	<u>1.94·10⁶</u>	<u>1.94·10⁶</u>	<u>1.94·10⁶</u>	<u>1.94·10⁶</u>
12	1.00	1.00	1.00	1.00	1.00	1.00	<u>1.94·10⁶</u>	<u>1.94·10⁶</u>	<u>1.94·10⁶</u>	<u>1.94·10⁶</u>	<u>1.94·10⁶</u>	<u>1.94·10⁶</u>
13	1.00	1.00	1.00	1.00	1.00	1.00	<u>1.94·10⁶</u>	<u>1.94·10⁶</u>	<u>1.94·10⁶</u>	<u>1.94·10⁶</u>	<u>1.94·10⁶</u>	<u>1.94·10⁶</u>
14	1.00	1.00	1.00	1.00	1.00	1.00	<u>1.94·10⁶</u>	<u>1.94·10⁶</u>	<u>1.94·10⁶</u>	<u>1.94·10⁶</u>	<u>1.94·10⁶</u>	<u>1.94·10⁶</u>
15	1.00	1.00	1.00	1.00	1.00	1.00	<u>1.94·10⁶</u>	<u>1.94·10⁶</u>	<u>1.94·10⁶</u>	<u>1.94·10⁶</u>	<u>1.94·10⁶</u>	<u>1.94·10⁶</u>



Table A5. Water classification parameters according to `water_type`. Underlined values are preliminary

Description	Class	Water temperature K	z_0 m	$z_{0,h}$ m	ϵ	albedo_type
lake	1	283	<u>0.01</u>	<u>0.001</u>	0.99	1
river	2	283	<u>0.01</u>	<u>0.001</u>	0.99	1
ocean	3	283	<u>0.01</u>	<u>0.001</u>	0.99	1
pond	4	283	<u>0.01</u>	<u>0.001</u>	0.99	1
fountain	5	283	<u>0.01</u>	<u>0.001</u>	0.99	1

Table A6. Soil classification parameters according to `soil_type`

Soil texture	Class	α_{vG}	l_{vG}	n_{vG}	$\gamma_{w,sat}$ $m\ s^{-1}$	m_{sat} $m^3\ m^{-3}$	m_{fc} $m^3\ m^{-3}$	m_{wilt} $m^3\ m^{-3}$	m_{res} $m^3\ m^{-3}$
coarse	1	3.83	1.150	1.38	$6.94 \cdot 10^{-6}$	0.403	0.244	0.059	0.025
medium	2	3.14	-2.342	1.28	$1.16 \cdot 10^{-6}$	0.439	0.347	0.151	0.010
medium-fine	3	0.83	-0.588	1.25	$0.26 \cdot 10^{-6}$	0.430	0.383	0.133	0.010
fine	4	3.67	-1.977	1.10	$2.87 \cdot 10^{-6}$	0.520	0.448	0.279	0.010
very fine	5	2.65	2.500	1.10	$1.74 \cdot 10^{-6}$	0.614	0.541	0.335	0.010
organic	6	1.30	0.400	1.20	$1.20 \cdot 10^{-6}$	0.766	0.663	0.267	0.010



Table A7. Surface albedo classification parameters according to `albedo_type`. Underlined values are preliminary

Class	Description	broadband	longwave	shortwave
ocean	1	0.06	0.06	0.06
mixed farming, tall grassland	2	0.19	0.28	0.09
tall/medium grassland	3	0.23	0.33	0.11
evergreen shrubland	4	0.23	0.33	0.11
short grassland/meadow/shrubland	5	0.25	0.34	0.14
evergreen needleleaf forest	6	0.14	0.22	0.06
mixed deciduous forest	7	0.17	0.27	0.06
deciduous forest	8	0.19	0.31	0.06
tropical evergreen broadleaved forest	9	0.14	0.22	0.06
medium/tall grassland/woodland	10	0.18	0.28	0.06
desert, sandy	11	0.43	0.51	0.35
desert, rocky	12	0.32	0.40	0.24
tundra	13	0.19	0.27	0.10
land ice	14	0.77	0.65	0.90
sea ice	15	0.77	0.65	0.90
snow	16	0.82	0.70	0.95
bare soil	17	0.08	0.08	0.08
asphalt/concrete mix	18	<u>0.17</u>	<u>0.17</u>	<u>0.17</u>
asphalt (asphalt concrete)	19	<u>0.17</u>	<u>0.17</u>	<u>0.17</u>
concrete (Portland concrete)	20	<u>0.30</u>	<u>0.30</u>	<u>0.30</u>
sett	21	<u>0.17</u>	<u>0.17</u>	<u>0.17</u>
paving stones	22	<u>0.17</u>	<u>0.17</u>	<u>0.17</u>
cobblestone	23	<u>0.17</u>	<u>0.17</u>	<u>0.17</u>
metal	24	<u>0.17</u>	<u>0.17</u>	<u>0.17</u>
wood	25	<u>0.17</u>	<u>0.17</u>	<u>0.17</u>
gravel	26	<u>0.17</u>	<u>0.17</u>	<u>0.17</u>
fine gravel	27	<u>0.17</u>	<u>0.17</u>	<u>0.17</u>
pebblestone	28	<u>0.17</u>	<u>0.17</u>	<u>0.17</u>
woodchips	29	<u>0.17</u>	<u>0.17</u>	<u>0.17</u>
tartan (sports)	30	<u>0.17</u>	<u>0.17</u>	<u>0.17</u>
artificial turf (sports)	31	<u>0.17</u>	<u>0.17</u>	<u>0.17</u>
clay (sports)	32	<u>0.17</u>	<u>0.17</u>	<u>0.17</u>
building	33	<u>0.17</u>	<u>0.17</u>	<u>0.17</u>

<https://doi.org/10.5194/gmd-2019-355>
Preprint. Discussion started: 4 May 2020
© Author(s) 2020. CC BY 4.0 License.



Appendix B: Look-up tables for various input data sources



Table B1. CLC classes to PALM vegetation type

CLC class number	description	PALM vegetation type ID
111	Continuous urban fabric	1
112	Discontinuous urban fabric	1
121	Industrial or commercial units	1
122	Road and rail networks and associated land	1
123	Port areas	1
124	Airports	3
131	Mineral extraction sites	1
132	Dump sites	1
133	Construction sites	1
141	Green urban areas	3
142	Sport and leisure facilities	3
211	Non-irrigated arable land	2
221	Vineyards	2
222	Fruit tree and berry plantations	2
231	Pasture, meadows and other permanent grasslands under agricultural use	3
242	Complex cultivation patterns	2
243	Land principally occupied by agriculture, with significant areas of natural vegetation	2
311	Broad-leaved forest	7
312	Coniferous forest	4
313	Mixed forest	17
321	Natural grassland	8
322	Moors and heathland	14
324	Transitional woodland/shrub	16
331	Beaches, dunes and sand plains	1
332	Bare rock	1
333	Sparsely vegetated areas	1
334	Burnt areas	1
335	Glaciers and perpetual snow	13
411	Inland marshes	14
412	Peatbogs	14
421	Coastal salt marshes	14
423	Intertidal flats	14



Table B2. OSM land use classes to PALM vegetation type

OSM label	PALM vegetation type ID
allotments	2
cemetery	3
commercial	255
farm	2
forest	17
grass	3
heath	3
industrial	255
meadow	3
military	1
orchard	3
park	3
quarry	1
recreation ground	3
residential	255
retail	255
scrub	16
vineyard	2



Table B3. Biotope type groups of the biotope map Hamburg to PALM vegetation type

Biotope group	Description (German)	PALM vegetation type ID
A	Ruderales und halbruderales Krautflur	3
B	Biotopkomplexe der Siedlungsflächen	1
E	Biotopkomplexe der Freizeit-, Erholungs-, Grünanlagen	3
G	Grünland - (§) (FFH 6510)	3
H	Gebüsche und Kleingehölze - (§) (FFH 91E0*)	16
K	Küstenbiotope - (§) (FFH 1140)	3
L	Biotope landwirtschaftlich genutzter Flächen	2
M	Hoch- und Übergangsmoore - (§) (FFH 7110*)	14
N	Biotope der Sümpfe und Niedermoore (gehölzfrei) - (§) (FFH 6431)	14
O	Offenbodenbiotope	1
T	Heiden, Borstgrasrasen, Magerrasen - (§) (FFH 4030)	3
V	Biotopkomplexe der Verkehrsflächen	3
W	Wald	17
Y	Biotope vegetationsarmer Flächen im Siedlungsbereich mit Spontanvegetation	1
Z	Vegetationsbestimmte Habitatstrukturen besiedelter Bereiche	1



Table B4. OSM pavement labels and according PALM pavement types

OSM pavement label	PALM pavement type	OSM pavement label	PALM pavement type
artificial turf	14	metal	7
asphalt	2	metal grid	7
asphalt:lanes	2	mud	15
asphalt;sett	2	paved	1
clay	15	paving stones	5
cobblestone	6	paving stones:30	5
cobblestone:flattened	6	pebblestone	11
cobblestone;asphalt	6	sand	10
compacted	16	sealed	1
concrete	3	sett	4
concrete:lanes	3	sett;paving stones	4
concrete:plates	3	stone	6
dirt	15	stone:plates	6
earth	15	tartan	13
fine gravel	10	undefined	1
grass	1	unknown pavement	1
grass paver	1	unpaved	10
gravel	9	wood	8
gravel:tracks	9	woodchips	12
ground	15		



Table B5. OSM road types and corresponding PALM pavement type. The street width in this table is only used to convert the line objects into areas if no value is indicated in the OSM data. If the number of lanes is indicated, the road width listed in Tab.B6 is applied.

OSM road type	buffer width	PALM pavement type
cycleway	2.5	asphalt
footway	2.5	paving stones
living street	5.5	paving stones
path	1.5	undefined
primary	7.5	asphalt
primary link	7.5	asphalt
residential	5.5	asphalt
secondary	6.5	asphalt
secondary link	6.5	asphalt
service	5.5	asphalt
tertiary	5.5	asphalt
tertiary link	5.5	asphalt
track	2.6	undefined
trunk	8	asphalt
trunk link	8	asphalt
unclassified	5.5	asphalt
motorway	0	asphalt
motorway link	0	asphalt



Table B6. Assumed road width when in OSM the number of lanes is indicated

Nr of lanes	buffer width
1	4
2	9
3	12
4	16
5	20
6	24



Table B7: Berlin ISU5 (Informationssystem Stadt und Umwelt, eng.: Informationssystem City and Surroundings) land use descriptions to PALM building type. The building function can be R = residential, O = other, X = no building. The age classes refer to the building period before 1951 (1), between 1951 and 2000 (2) and after 2000 (3). The combination of the function and the building age according to Tab. A2 results in the PALM building type.

ISU5 land use description	Function	Age	Building type
Allotment garden	R	2	2
Fallow area	X	0	0
Commercial and industrial area, large-scale retail, sparse development	O	2	5
Commercial and industrial area, large-scale retail, dense development	O	2	5
Security and order	O	2	5
Body of water	X	0	0
Heterogeneous inner-city mixed development, post-war gap closure	R	2	2
De-cored block development, post-war gap closure	R	2	2
New school (built after 1945)	O	2	5
Culture	O	2	5
Closed block development, rear courtyard (1870s - 1918), 5-storey	R	1	1
Dense block development, closed rear courtyard (1870s- 1918), 5 - 6-storey	R	1	1
City square / promenade	X	0	0
Block-edge development with large quadrangles (1920s - 1940s), 2 - 5-storey	R	1	1
Park / green space	X	0	0
Railway station and railway ground, without track area	X	0	0
Free row development, landscaped residential greenery (1950s - 1970s), 2 - 6-storey	R	2	2
Old school (built before 1945)	O	1	4
Parking area	X	0	0
Church	O	1	4
Track area	X	0	0



Children's day care centre	O	2	5
Core area	R	2	2
University and research	O	2	5
Cemetery	X	0	0
Administrative	O	2	5
Non-residential mixed use area, dense develop- ment	O	2	5
Utility area	O	2	5
Other and miscellaneous public facility / special use area	O	2	5
Sport facility, uncovered	X	0	0
Rental-flat buildings of the 1990s and later	R	2	2
Non-residential mixed use area, sparse develop- ment	O	2	5
Forest	X	0	0
Densification in single-family home area, mixed development with yard and semi-private greening (1870s to present)	R	1	4
Other youth facility	O	2	5
Detached single-family homes with yards	R	2	2
Large estate with tower high-rise buildings (1960s - 1990s), 4 - 11-storey and more	R	2	2
Row houses and duplex with yards	R	2	2
Sport facility, covered	O	2	5
Villas and town villas with park-like gardens (mostly 1870s- 1945)	R	1	1
Other traffic area	X	0	0
Hospital	O	2	5
Tree nursery / horticulture	X	0	0
Parallel row buildings with architectural green strips (1920s - 1930s), 2 - 5 storey	R	1	1
Weekend cottage and allotment-garden-type area	R	2	2
Closed and semi-open block development, decora- tive and garden courtyard (1870s - 1918), 4-storey	R	1	1
Construction site	X	0	0



Mixed development, semi-open and open shed courtyard, 2 - 4-storey	O	2	5
Village-like mixed development	O	2	5
Agriculture	X	0	0
Airport	O	2	5
Camping ground	X	0	0

Table B8: ALKIS land use descriptions to PALM building type. The building function can be R = residential, O = other, X = no building. The combination of the function and the building age according to Tab. A2 results in the PALM building type.

ALKIS ID	land use description (German)	Function
1000	Wohngebäude	R
1010	Wohnhaus	R
1020	Wohnheim	R
1022	Seniorenheim	R
1024	Studenten-, Schülerwohnheim	R
1025	Schullandheim	R
1100	Gemischt genutztes Gebäude mit Wohnen	R
1110	Wohngebäude mit Gemeinbedarf	R
1120	Wohngebäude mit Handel und Dienstleistungen	R
1121	Wohn- und Verwaltungsgebäude	R
1122	Wohn- und Bürogebäude	R
1123	Wohn- und Geschäftsgebäude	R
1130	Wohngebäude mit Gewerbe und Industrie	R
1131	Wohn- und Betriebsgebäude	R
1210	Land- und forstwirtschaftliches Wohngebäude	R
1220	Land- und forstwirtschaftliches Wohn- und Betriebsgebäude	R
1222	Wohn- und Wirtschaftsgebäude	R
1223	Forsthaus	O
1310	Gebäude zur Freizeitgestaltung	O
1311	Ferienhaus	R



1312	Wochenendhaus	R
1313	Gartenhaus	R
2000	Gebäude für Wirtschaft oder Gewerbe	O
2010	Gebäude für Handel und Dienstleistungen	O
2020	Bürogebäude	O
2030	Kreditinstitut	O
2040	Versicherung	O
2050	Geschäftsgebäude	O
2051	Kaufhaus	O
2052	Einkaufszentrum	O
2053	Markthalle	O
2054	Laden	O
2055	Kiosk	O
2060	Messehalle	O
2071	Hotel, Motel, Pension	O
2072	Jugendherberge	O
2074	Campingplatzgebäude	O
2080	Gebäude für Bewirtung	O
2081	Gaststätte, Restaurant	O
2083	Kantine	O
2090	Freizeit- und Vergnügungsstätte	O
2092	Kino	O
2094	Spielkasino	O
2100	Gebäude für Gewerbe und Industrie	O
2110	Produktionsgebäude	O
2111	Fabrik	O
2112	Betriebsgebäude	O
2120	Werkstatt	O
2130	Tankstelle	O
2131	Waschstraße, Waschanlage, Waschhalle	O
2140	Gebäude für Vorratshaltung	O
2141	Kühlhaus	O
2142	Speichergebäude	O
2143	Lagerhalle, Lagerschuppen, Lagerhaus	O
2150	Speditonsgebäude	O



2160	Gebäude für Forschungszwecke	O
2180	Gebäude für betriebliche Sozialeinrichtung	O
2200	Sonstiges Gebäude für Gewerbe und Industrie	O
2213	Schöpfwerk	O
2310	Gebäude für Handel und Dienstleistung mit Wohnen	O
2320	Gebäude für Gewerbe und Industrie mit Wohnen	O
2400	Betriebsgebäude zu Verkehrsanlagen (allgemein)	O
2410	Betriebsgebäude für Straßenverkehr	O
2411	Straßenmeisterei	O
2412	Wartehalle	O
2420	Betriebsgebäude für Schienenverkehr	O
2422	Lokschuppen, Wagenhalle	O
2430	Betriebsgebäude für Flugverkehr	O
2431	Flugzeughalle	O
2440	Betriebsgebäude für Schiffsverkehr	O
2441	Werft (Halle)	O
2443	Betriebsgebäude zur Schleuse	O
2444	Bootshaus	O
2460	Gebäude zum Parken	O
2461	Parkhaus	O
2462	Parkdeck	O
2463	Garage	O
2464	Fahrzeughalle	O
2465	Tiefgarage	X
2500	Gebäude zur Versorgung	O
2501	Gebäude zur Energieversorgung	O
2510	Gebäude zur Wasserversorgung	O
2512	Pumpstation	O
2513	Wasserbehälter	X
2520	Gebäude zur Elektrizitätsversorgung	O
2521	Elektrizitätswerk	O
2522	Umspannwerk	O
2523	Umformer	X
2528	Turbinenhaus	O



2529	Kesselhaus	O
2540	Gebäude für Fernmeldewesen	O
2560	Gebäude an unterirdischen Leitungen	O
2570	Gebäude zur Gasversorgung	O
2580	Heizwerk	O
2590	Gebäude zur Versorgungsanlage	O
2600	Gebäude zur Entsorgung	O
2611	Gebäude der Kläranlage	O
2612	Toilette	O
2620	Gebäude zur Abfallbehandlung	O
2621	Müllbunker	O
2622	Gebäude zur Müllverbrennung	O
2700	Gebäude für Land- und Forstwirtschaft	O
2720	Land- und forstwirtschaftliches Betriebsgebäude	O
2721	Scheune	O
2723	Schuppen	O
2724	Stall	O
2726	Scheune und Stall	O
2728	Reithalle	O
2729	Wirtschaftsgebäude	O
2740	Treibhaus, Gewächshaus	O
2741	Treibhaus	O
2742	Gewächshaus, verschiebbar	O
3000	Gebäude für öffentliche Zwecke	O
3010	Verwaltungsgebäude	O
3012	Rathaus	O
3013	Post	O
3014	Zollamt	O
3015	Gericht	O
3016	Botschaft, Konsulat	O
3019	Finanzamt	O
3020	Gebäude für Bildung und Forschung	O
3021	Allgemein bildende Schule	O
3022	Berufsbildende Schule	O
3023	Hochschulgebäude (Fachhochschule, Universität)	O



3024	Forschungsinstitut	O
3030	Gebäude für kulturelle Zwecke	O
3031	Schloss	O
3032	Theater, Oper	O
3033	Konzertgebäude	O
3034	Museum	O
3035	Rundfunk, Fernsehen	O
3036	Veranstaltungsgebäude	O
3037	Bibliothek, Bücherei	O
3040	Gebäude für religiöse Zwecke	O
3041	Kirche	O
3042	Synagoge	O
3043	Kapelle	O
3044	Gemeindehaus	O
3045	Gotteshaus	O
3046	Moschee	O
3048	Kloster	O
3050	Gebäude für Gesundheitswesen	O
3051	Krankenhaus	O
3052	Heilanstalt, Pflegeanstalt, Pflegestation	O
3053	Ärztehaus, Poliklinik	O
3060	Gebäude für soziale Zwecke	O
3061	Jugendfreizeitheim	O
3062	Freizeit-, Vereinsheim, Dorfgemeinschafts-, Bürgerhaus	O
3065	Kinderkrippe, Kindergarten, Kindertagesstätte	O
3070	Gebäude für Sicherheit und Ordnung	O
3071	Polizei	O
3072	Feuerwehr	O
3073	Kaserne	O
3074	Schutzbunker	O
3075	Justizvollzugsanstalt	O
3080	Friedhofsgebäude	O
3081	Trauerhalle	O
3082	Krematorium	O



3090	Empfangsgebäude	O
3091	Bahnhofsgebäude	O
3092	Flughafengebäude	O
3097	Gebäude zum Busbahnhof	O
3098	Empfangsgebäude Schifffahrt	O
3100	Gebäude für öffentliche Zwecke mit Wohnen	O
3200	Gebäude für Erholungszwecke	O
3210	Gebäude für Sportzwecke	O
3211	Sport-, Turnhalle	O
3212	Gebäude zum Sportplatz	O
3220	Badegebäude	O
3221	Hallenbad	O
3222	Gebäude im Freibad	O
3230	Gebäude im Stadion	O
3240	Gebäude für Kurbetrieb	O
3260	Gebäude im Zoo	O
3270	Gebäude im botanischen Garten	O
3281	Schutzhütte	O
3290	Touristisches Informationszentrum	O
9998	unbekannt	U
11161	Jugendhaus	O
11162	Waldheim	R
11491	Vereinsheim	O
12359	Aufzug	X
12619	Rückhaltebecken	X
12629	Kamin	X
19702	Wasserturm	X
19703	Kirchturm, Glockenturm	O
19704	Aussichtsturm	O
19705	Sende-, Funk-, Fernmeldeturm	X
19706	Stadt-, Torturm	X
19901	Überdachung	X
19902	Unterkellerung	X



Table B9. OSM values to PALM water type

OSM label	PALM water type ID
canal	2
ditch	2
drain	255
fountain	5
lake	1
pond	4
reflection-pool	4
reservoir	1
river	2
riverbank	2
stream	2
(null)	255
Brack	4
Teich	4
See	1
Weiher	4
Moor	255



Table B10. CLC classes to PALM water type

CLC class number	description	PALM water type ID
511	Water courses	2
512	Water bodies	1
521	Coastal lagoons	3
522	Estuaries	3
523	Sea and ocean	3



Table B11: Biotope types of Hamburg to PALM water type

Biotope abbreviation	Description (German)	PALM water type ID
FBA	Bach, ausgebaut	2
FBM	Bach, naturnah mit Beeinträchtigungen/Verbauungen - (§) (FFH 3260)	2
FBR	Bach, weitgehend naturnah	2
FBS	Aufgestauter Bachabschnitt	2
FBT	Bach-Altarm	2
FFA	Fluss, ausgebaut	2
FFF	Flachwasserbereiche der Elbe	2
FFM	Fluss, naturnah mit Beeinträchtigungen/Verbauungen	2
FFR	Fluss, weitgehend naturnah	2
FFS	Aufgestauter Flussabschnitt	2
FFT	Fluss-Altarm	2
FG	Graben mit Stillgewässercharakter	4
FGA	Nährstoffarmer Graben mit Stillgewässercharakter	4
	-	
FGM	Graben mittlerer Nährstoffgehalte mit Stillgewässercharakter - (§)	4
FGR	Nährstoffreicher Graben mit Stillgewässercharakter	4
FGV	Nährstoffreicher Graben mit Stillgewässercharakter	4
FGX	Abwassergraben	2
FH	Hafenbecken	1
FK	Kanal	2
FLH	Wettern, Hauptgraben	2
FLM	Graben mittlerer Nährstoffgehalte mit Fließgewässercharakter	2
FLR	Nährstoffreicher Graben mit Fließgewässercharakter	2
FQ	Quellbereich -	4
FQG	Tümpelquelle - §	4



FQS	Tümpelquelle - §	4
FSO	Flussstrand, gestört - (§)	255
FSV	Flussstrand, naturnah -	255
FSW	Strandwall am Elbufer -	255
FWB	Flusswatt mit Pioniervegetation -	2
FWO	Flusswatt, ohne Bewuchs	2
FWP	Priel	2
FWV	Tideröhricht	2
FWX	Verbautes Elbufer mit naturnahen Vegetations- elementen	255
FWZ	Sonstige naturnahe Flächen im Wasserwechsel- bereich der tide beeinflussten Flussunterläufe	255
SEA	Abbaugewässer, klein, naturnah, nährstoffreich	4
SEB	Brack, naturnah, nährstoffreich	4
SED	Bombentrichter, naturnah, nährstoffreich	4
SEF	Altwasser, klein, naturnah	4
SEG	Angelegte Kleingewässer, klein, naturnah, nährstoffreich - § FFH 3150 18	4
SEN	Natürliches, nährstoffreiches Kleingewässer	4
SEO	Nährstoffreiche Kleingewässer ohne Bewuchs	4
SER	Naturnahes, nährstoffreiches Regenrückhalte- becken	4
SES	Nährstoffreiche Kleingewässer mit artenarmem Bewuchs	4
SET	Teich, nährstoffreich, naturnah	4
SEW	Weidekuhle, nährstoffreich, naturnah	4
SEY	Beregnungsbecken mit naturnahen Elementen	4
SEZ	Sonstiges, naturnahes, nährstoffreiches Kleingewässer	4
SGA	Abbaugewässer, Baggersee, groß	1
SGF	Altwasser, groß	1
SGT	Staugewässer, groß	1
SGZ	Sonstiges Stillgewässer, groß	1
SOA	Abbaugewässer, naturnah, nährstoffarm	4
SOG	Angelegtes Kleingewässer, naturnah, nährstoffarm	4



SOM	Moorgewässer, naturnah, nährstoffarm	4
SON	Kleingewässer natürlicher Entstehung, naturnah, nährstoffarm	4
SOT	Teich, nährstoffarm, naturnah	4
STA	Ackertümpel	4
STG	Wiesen- oder Weidetümpel	4
STR	Rohbodentümpel	4
STW	Waldtümpel	4
STZ	Sonstiger Tümpel	4
SX	Naturfernes Stillgewässer	4
SXA	Naturfernes Abbaugewässer	4
SXB	Sonstiges Brack	4
SXG	Naturfernes Ziergewässer	4
SXK	Klärteich, Absetzbecken	4
SXL	Löschwasserbecken, naturfern	4
SXP	Fischteich, naturfern	4
SXR	Rückhaltebecken, naturfern	4
SXT	Teich, naturfern	4
SXY	Beregnungsbecken, naturfern	4
SXZ	Sonstiges, naturfernes Wasserbecken	4



Author contributions. BM, MS and FKS designed the input data requirements for PALM. MS implemented the data input and the PALM-internal data processing. BM developed the `palm_csd` code and created the static driver in the supplements based on the input data of Berlin provided by WH and JZ. WH and JZ generated the input data for Berlin, Stuttgart and Hamburg shown in the manuscript. WH and BM prepared the manuscript with contributions of MS, JZ, DP, CB and TE

5 *Competing interests.* The authors declare that they have no conflict of interest.

Acknowledgements. The work presented in this paper was funded by the German Federal Ministry of Education and Research (BMBF) under grant 01LP1601 within the framework of Research for Sustainable Development (FONA; www.fona.de), which is greatly acknowledged. We thank R. Kapp (Amt für Umweltschutz) and J. Oberdorfer (Stadtvermessungsamt) of the Landeshauptstadt Stuttgart, Germany for providing the municipal data of Stuttgart.



References

- Arbeitsgemeinschaft der Vermessungsverwaltungen der Länder der Bundesrepublik Deutschland: 3D-Gebäudemodelle LoD1: Produktblatt, <http://www.adv-online.de/AdV-Produkte/Standards-und-Produktblaetter/Produktblaetter/binarywriterservlet?imgUid=fbe60187-4fe3-2b41-6ad4-1fd3072e13d6&uBasVariant=11111111-1111-1111-1111-111111111111>, a.
- 5 Arbeitsgemeinschaft der Vermessungsverwaltungen der Länder der Bundesrepublik Deutschland: 3D-Gebäudemodelle LoD2: Produktblatt, <http://www.adv-online.de/AdV-Produkte/Standards-und-Produktblaetter/binarywriterservlet?imgUid=e9e60187-4fe3-2b41-6ad4-1fd3072e13d6&uBasVariant=11111111-1111-1111-1111-111111111111>, b.
- Baghdadi, N. and Zribi, M., eds.: Optical remote sensing of land surfaces: Techniques and methods, Remote Sensing Observations of Continental Surfaces Set, Elsevier and ISTE Press, Oxford and London, <https://doi.org/10.1016/C2015-0-01220-5>, 2016.
- 10 Bohrer, G., Wolosin, M., Brady, R., and Avissar, R.: A virtual canopy generator (V-CaGe) for modelling complex heterogeneous forest canopies at high resolution, *Tellus*, 59B, 566–576, <https://doi.org/10.1111/j.1600-0889.2007.00253.x>, 2007.
- Esch, T., Üreyen, S., Zeidler, J., Metz–Marconcini, A., Hirner, A., Asamer, H., Tum, M., Böttcher, M., Kuchar, S., Svaton, V., and Marconcini, M.: Exploiting big earth data from space – first experiences with the timescan processing chain, *Big Earth Data*, 2, 36–55, <https://doi.org/10.1080/20964471.2018.1433790>, 2018.
- 15 European Union, Copernicus Land Monitoring Service 2017, E. E. A. E.: CORINE Land Cover 2012 100 m, <https://land.copernicus.eu/pan-european/corine-land-cover>, 2017.
- Farr, T. G., Rosen, P. A., Caro, E., Crippen, R., Duren, R., Hensley, S., Kobrick, M., Paller, M., Rodriguez, E., Roth, L., Seal, D., Shaffer, S., Shimada, J., Umland, J., Werner, M., Oskin, M., Burbank, D., and Alsdorf, D.: The Shuttle Radar Topography Mission, *Reviews of Geophysics*, 45, <https://doi.org/10.1029/2005RG000183>, 2007.
- 20 Fassnacht, F. E., Latifi, H., Stereńczak, K., Modzelewska, A., Lefsky, M., Waser, L. T., Straub, C., and Ghosh, A.: Review of studies on tree species classification from remotely sensed data, *Remote Sensing of Environment*, 186, 64–87, <https://doi.org/10.1016/j.rse.2016.08.013>, 2016.
- GDAL/OGR contributors: GDAL/OGR Geospatial Data Abstraction software Library, <http://gdal.org>, 2019.
- Graser, A., Straub, M., and Dragaschnig, M.: Is OSM Good Enough for Vehicle Routing? A Study Comparing Street Networks in Vienna, in: *Progress in Location-Based Services 2014*, edited by Gartner, G. and Huang, H., pp. 3–17, Springer International Publishing, Cham, https://doi.org/10.1007/978-3-319-11879-6_1, 2015.
- 25 Gronemeier, T. and Sühling, M.: On the effects of lateral openings on courtyard ventilation and pollution – a large-eddy simulation study, *Atmosphere (Basel)*, 10, 63, <https://doi.org/10.3390/atmos10020063>, 2019.
- Haklay, M.: How Good is Volunteered Geographical Information? A Comparative Study of OpenStreetMap and Ordnance Survey Datasets, *Environment and Planning B: Planning and Design*, 37, 682–703, <https://doi.org/10.1068/b35097>, 2010.
- 30 Kanani-Sühling, F. and Raasch, S.: Spatial Variability of Scalar Concentrations and Fluxes Downstream of a Clearing-to-Forest Transition: A Large-Eddy Simulation Study, *Boundary-Layer Meteorology*, 155, 1–27, <https://doi.org/10.1007/s10546-014-9986-3>, 2015.
- Khatami, R., Mountrakis, G., and Stehman, S. V.: A meta-analysis of remote sensing research on supervised pixel-based land-cover image classification processes: General guidelines for practitioners and future research, *Remote Sensing of Environment*, 177, 89–100, <https://doi.org/10.1016/j.rse.2016.02.028>, 2016.
- 35 Kurppa, M., Hellsten, A., Auvinen, M., Raasch, S., Vesala, T., and Järvi, L.: Ventilation and Air Quality in City Blocks Using Large-Eddy Simulation—Urban Planning Perspective, *Atmosphere (Basel)*, 9, 65, <https://doi.org/10.3390/atmos9020065>, 2018.



- Lo, K. W. and Ngan, K.: Characterizing Ventilation and Exposure in Street Canyons Using Lagrangian Particles, *J. Appl. Meteorol. Climatol.*, 56, 1177–1194, <https://doi.org/10.1175/JAMC-D-16-0168.1>, 2017.
- Ma, S., Zhou, Y., Gowda, P. H., Dong, J., Zhang, G., Kakani, V. G., Wagle, P., Chen, L., Flynn, K. C., and Jiang, W.: Application of the water-related spectral reflectance indices: A review, *Ecological Indicators*, 98, 68–79, <https://doi.org/10.1016/j.ecolind.2018.10.049>, 2019.
- 5 Markkanen, T., Rannik, Ü., Marcolla, B., Cescatt, A., and Vesala, T.: Footprints and fetches for fluxes over forest canopies with varying structure and density, *Boundary-Layer Meteorol.*, 106, 437–459, 2003.
- Maronga, B., Banzhaf, S., Burmeister, C., Esch, T., Forkel, R., Fröhlich, D., Fuka, V., Gehrke, K., Geletic, J., Giersch, S., Gronemeier, T., Groß, G., Heldens, W., Hellsten, A., Hoffmann, F., Inagaki, A., Kadasch, E., Kanani-Sühring, F., Ketelsen, K., Khan, B. A., Knigge, C., Knoop, H., Krc, P., Kurppa, M., Maamari, H., Matzarakis, A., Mauder, M., Pallasch, M., Pavlik, D., Pfafferott, J., Resler, J., Rissmann, S.,
- 10 Russo, E., Salim, M., Schrempf, M., Schwenkel, J., Seckmeyer, G., Schubert, S., Sühring, M., von Tils, R., Vollmer, L., Ward, S., Witha, B., Wurps, H., Zeidler, J., and Raasch, S.: Overview of the PALM model system 6.0, *Geosci. Model Dev. Discuss.*, submitted, 2019.
- Masson, V., Heldens, W., Bocher, E., Bonhomme, M., Bucher, B., Burmeister, C., de Munck, C., Esch, T., Hidalgo, J., Kanani-Sühring, F., Kwok, Y.-T., Lemonsu, A., Lévy, J.-P., Maronga, B., Pavlik, D., Petit, G., See, L., Schoetter, R., Tornay, N., Votsis, A., and Zeidler, J.: City-descriptive input data for urban climate models: Model requirements, data sources and challenges, *Urban Climate*, 31, 100536,
- 15 <https://doi.org/10.1016/j.uclim.2019.100536>, 2020.
- Open Geospatial Consortium: City Geography Markup Language (CityGML) Encoding Standard, version: 2.0.0, <http://www.opengis.net/spec/citygml/2.0>, 2012.
- Quinn, S. and Bull, F.: Understanding Threats to Crowdsourced Geographic Data Quality Through a Study of OpenStreetMap Contributor Bans., in: *Geospatial information system use in public organizations*, ROUTLEDGE, New York, 2019.
- 20 Resler, J., Krč, P., Belda, M., Juruš, P., Benešová, N., Lopata, J., Vlček, O., Damašková, D., Eben, K., Derbek, P., Maronga, B., and Kanani-Sühring, F.: PALM-USM v1.0: A new urban surface model integrated into the PALM large-eddy simulation model, *Geoscientific Model Development*, 10, 3635–3659, <https://doi.org/10.5194/gmd-10-3635-2017>, 2017.
- Rizzoli, P., Martone, M., Gonzalez, C., Wecklich, C., Borla Tridon, D., Bräutigam, B., Bachmann, M., Schulze, D., Fritz, T., Huber, M., Wessel, B., Krieger, G., Zink, M., and Moreira, A.: Generation and performance assessment of the global TanDEM-X digital elevation
- 25 model, *ISPRS Journal of Photogrammetry and Remote Sensing*, 132, 119–139, <https://doi.org/10.1016/j.isprsjprs.2017.08.008>, 2017.
- Roessner, S., Segl, K., Heiden, U., and Kaufmann, H.: Automated differentiation of urban surfaces based on airborne hyperspectral imagery, *IEEE Transactions on Geoscience and Remote Sensing*, 39, 1525–1532, <https://doi.org/10.1109/36.934082>, 2001.
- Rouse, J. W., J., Haas, R. H., Schell, J. A., and Deering, D. W.: Monitoring Vegetation Systems in the Great Plains with Erts, vol. 351, p. 309, 1974.
- 30 Scherer, D., Antretter, F., Bender, S., Cortekar, J., Emeis, S., Fehrenbach, U., Gross, G., Halbig, G., Hasse, J., Maronga, B., Raasch, S., and Scherber, K.: Urban Climate Under Change [UC]2 ? A National Research Programme for Developing a Building-Resolving Atmospheric Model for Entire City Regions, *Meteorologische Zeitschrift*, 28, 95–104, <https://doi.org/10.1127/metz/2019/0913>, 2019.
- Sharma, A., Woodruff, S., Budhathoki, M., Hamlet, A. F., Chen, F., and Fernando, H. J. S.: Role of green roofs in reducing heat stress in vulnerable urban communities—a multidisciplinary approach, *Environmental Research Letters*, 13, 094011, <https://doi.org/10.1088/1748-9326/aad93c>, 2018.
- 35 van der Linden, S., Okujeni, A., Canters, F., Degerickx, J., Heiden, U., Hostert, P., Priem, F., Somers, B., and Thiel, F.: Imaging Spectroscopy of Urban Environments, *Surveys in Geophysics*, 40, 471–488, <https://doi.org/10.1007/s10712-018-9486-y>, 2019.



- Verrelst, J., Camps-Valls, G., Muñoz-Marí, J., Rivera, J. P., Veroustraete, F., Clevers, J. G., and Moreno, J.: Optical remote sensing and the retrieval of terrestrial vegetation bio-geophysical properties – A review, *ISPRS Journal of Photogrammetry and Remote Sensing*, 108, 273–290, <https://doi.org/10.1016/j.isprsjprs.2015.05.005>, 2015.
- Wang, Q., Adiku, S., Tenhunen, J., and Granier, A.: On the relationship of NDVI with leaf area index in a deciduous forest site, *Remote Sens. Env.*, 94, 244–255, 2005.
- Working Committee of the Surveying Authorities of the States of the Federal Republic of Germany, .: Documentation on the Modelling of Geoinformation of Official Surveying and Mapping, <http://www.adv-online.de/Publications/AFIS-ALKIS-ATKIS-Project/>, 2015.
- Wulder, M. A., Coops, N. C., Roy, D. P., White, J. C., and Hermosilla, T.: Land cover 2.0, *International Journal of Remote Sensing*, 39, 4254–4284, <https://doi.org/10.1080/01431161.2018.1452075>, 2018.
- 10 Yan, W. Y., Shaker, A., and El-Ashmawy, N.: Urban land cover classification using airborne LiDAR data: A review, *Remote Sensing of Environment*, 158, 295–310, <https://doi.org/10.1016/j.rse.2014.11.001>, 2015.



Table 12. List of LOD1 variables that can be specified in the static driver file.

Variable name	Dimensions	NetCDF data type	Values/Units	Description
albedo_type	(y, x)	NC_BYTE	0 – 18	Optional classification of albedo. Default values are set by building_type, pavement_type, pavement_type, vegetation_type, and water_type but will be overwritten in case albedo_type is defined
buildings_2d	(y, x)	NC_FLOAT	m	Building height relative to underlying terrain. Requires setting of building id
buildings_id	(y, x)	NC_INT	-	Building id, used to identify single building envelopes for mapping of buildings on complex terrain
building_type	(y, x)	NC_BYTE	0 – 6	Bulk classification of building types
pavement_type	(y, x)	NC_BYTE	0 – 16	Bulk classification of pavements on soil. Requires setting of a soil type
surface_fraction	(n, y, x)	NC_FLOAT	0 – 1	Relative fraction of the respective surface type given via vegetation_type ($n = 0$), pavement_type ($n = 1$) and water_type ($n = 2$). The sum over all relative fractions must be equal to one for each location. Note that more than one surface type per pixel are currently not supported by PALM
vegetation_type	(y, x)	NC_BYTE	0 – 18	Bulk classification of non-resolved vegetation surfaces at natural land surface types. Requires setting of a soil type
water_type	(y, x)	NC_BYTE	0 – 18	Bulk classification of water bodies
zt	(y, x)	NC_FLOAT	m	Terrain height above mean sea level



Table 13. List of LOD2 variables that can be specified in the static driver file.

Variable name	Dimensions	NetCDF data type	n	Description
albedo_pars	(n, y, x)	NC_FLOAT	0 – 7	Optional classification of individual albedo values for broadband, longwave, and shortwave radiation for each pixel (y, x) . See Tab. S8 in the Supplements
buildings_3d	(z, y, x)	NC_BYTE	0-1	Three-dimensional building topology relative to underlying terrain in which setting of 1 refers to building and 0 refers to no building. The z -dimension only needs to be large enough to embrace the building topology
building_pars	(n, z_{wall}, y, x)	NC_FLOAT	0 – 46	Optional setting of building material parameters for each wall layer z_{wall} and pixel (y, x) . See Tab. S9 in the Supplements
building_surface_pars	(n, y, x)	NC_FLOAT	0 – 46	Optional setting of building surface parameters for each pixel (y, x) . See Tab. S10 in the Supplements
pavement_pars	(n, z_{soil}, y, x)	NC_FLOAT	$n = 0 - 1$	Optional setting of pavement thermal parameters for each soil layer z_{soil} and pixel (y, x) . See Tab. S11 in the Supplements
pavement_surface_pars	(n, y, x)	NC_FLOAT	$n = 0 - 3$	Optional setting of pavement surface parameters for each pixel (y, x) . See Tab. S12 in the Supplements
root_fraction	(z_{soil}, y, x)	NC_FLOAT	$n = 0 - 1$	Root fraction within the individual soil layers z_{soil}
soil_pars	(n, z_{soil}, y, x)	NC_FLOAT	$n = 0 - 8$	Optional setting of soil parameters for each soil layer z_{soil} and pixel (y, x) . See Tab. S13 in the Supplements
vegetation_pars	(n, y, x)	NC_FLOAT	$n = 0 - 11$	Optional setting of vegetation parameters for each pixel (y, x) . See Tab. S14 in the Supplements
water_pars	(n, y, x)	NC_FLOAT	$n = 0 - 6$	Optional setting of water body parameters for each pixel (y, x) . See Tab. S15 in the Supplements



Table 14. List of LOD3 variables that can be specified in the static driver file.

Variable name	Dimensions	NetCDF data type	n	Description
building_surface_pars	(n, z, y, x)	NC_FLOAT	0 – 46	Optional setting of building surface parameters for each surface height z and each surface pixel location (y, x) . See Tab. S10 in the Supplements



Table 15. List of LOD4 variables that can be specified in the static driver file.

Variable name	Dimensions	NetCDF data type	n	Description
building_pars	(n, z_{wall}, s)	NC_FLOAT	0 – 46	Optional setting of building material parameters for each wall layer z_{wall} and each surface element s . See Tab. S9 in the Supplements
building_surface_pars	(n, s)	NC_FLOAT	0 – 46	Optional setting of building surface parameters for each surface element s . See Tab. S10 in the Supplements



Table 16. List and average properties of the most common street trees in Berlin.

Genus Unit	Quantity	Tree height m	Crown diameter m	Trunk diameter (DBH) m	Age yr
Acer	119863	12.1	7.1	1.0	41.8
Aesculus	24601	12.2	7.0	1.3	51.3
Ailanthus	1833	14.2	8.5	1.3	46.4
Alnus	3764	16.3	5.9	1.3	47.9
Betula	25580	14.0	6.0	1.0	39.7
Carpinus	15862	10.2	6.0	0.8	33.9
Corylus	7789	8.8	4.9	0.7	29.6
Crataegus	8570	5.9	3.5	0.5	26.2
Fagus	9923	17.5	9.9	1.7	91.3
Fraxinus	14217	10.7	5.6	0.9	35.1
Ginkgo	1289	8.4	4.0	0.6	24.8
Gleditsia	2746	10.6	6.3	0.8	29.3
Juglans	1124	9.5	6.8	0.9	37.2
Larix	1218	16.7	7.1	1.2	51.3
Malus	3146	4.8	3.5	0.5	21.5
Picea	3122	13.6	3.6	0.9	37.5
Pinus	13985	15.7	6.3	1.2	49.2
Platanus	25548	14.7	9.9	1.4	50.6
Populus	16750	20.6	8.8	1.7	54.9
Prunus	14594	7.0	4.9	0.7	27.8
Pseudotsuga	2652	17.6	5.8	1.2	42.8
Pyrus	2779	6.0	2.6	0.4	19.9
Quercus	58416	14.2	8.0	1.3	55.6
Robinia	20341	13.9	6.7	1.1	42.4
Salix	4891	13.8	7.9	1.6	44.5
Sophora	1852	10.2	7.7	1.0	36.9
Sorbus	8251	6.7	4.0	0.6	28.2
Taxus	2767	7.6	5.2	0.8	43.3
Tilia	156496	12.6	7.2	1.1	45.7
Ulmus	8729	13.8	7.4	1.2	42.2